GEOPOLYMER IN SELF-SENSING APPLICATIONS

CHENMENG ZHANG

PHD CANDIDATE IN CIVIL ENGINEERING

UNIVERSITY OF SURREY

2025.07.08.

GEOPOLYMER CAMP 2025

UNIVERSITY OF SURREY

About me

2014-2018

2018-2020

BEng in civil engineering (Architecture), Yangtze University, China

MSc in structural engineering, Cardiff University, UK

BIM (second prize in 4TH Luban cup national graduation competition(team leader))

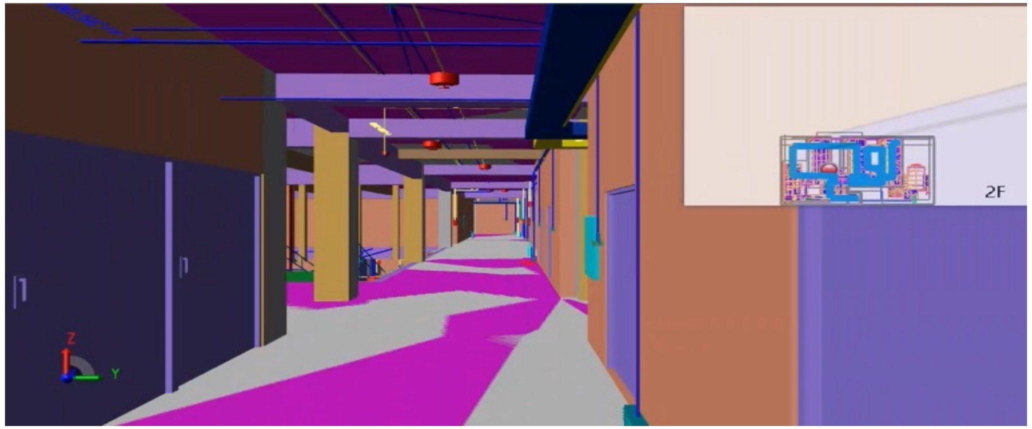

Self-compacting concrete
SPH simulation

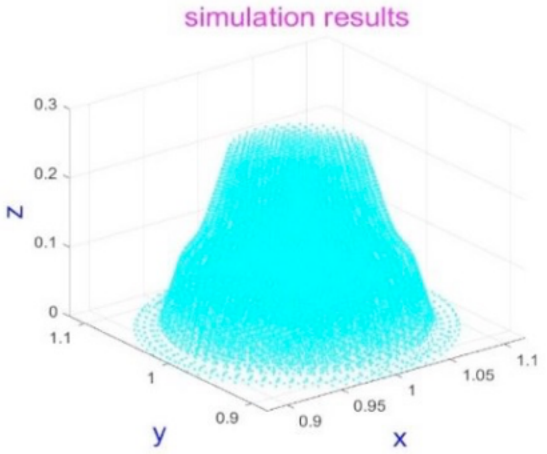

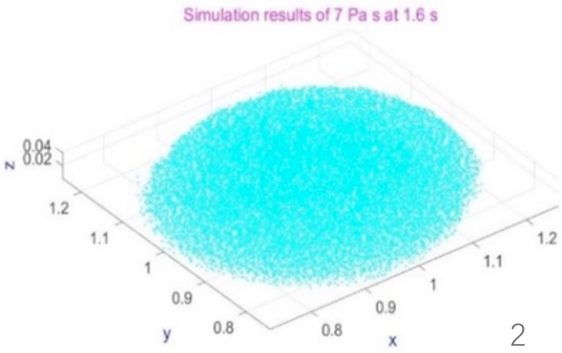

About me

2019-2021

Structural engineer and project manager, Shenzhen, Shanghai & Hubei, China

2021-2025

PhD candidate in civil and environmental engineering, University of Surrey, UK

High-rise building
Residential building

Associate constructor certification (Hubei)

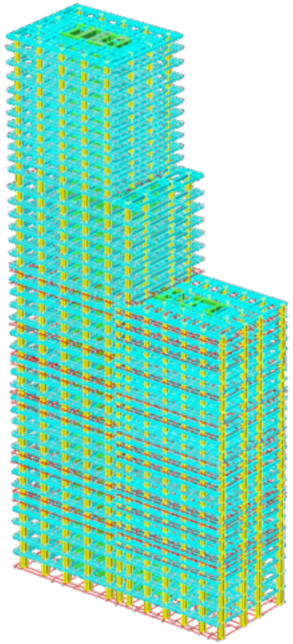

Alkali-activated materials
Self-sensing materials

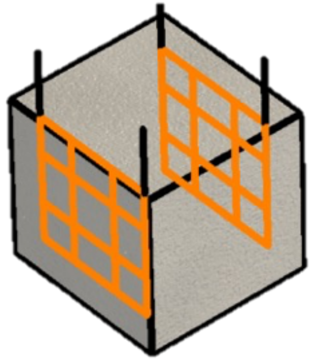

GEOPOLYMER IN SELF-SENSING APPLICATIONS

CHENMENG ZHANG

PHD CANDIDATE IN CIVIL ENGINEERING

UNIVERSITY OF SURREY

2025.07.08.

GEOPOLYMER CAMP 2025

UNIVERSITY OF SURREY

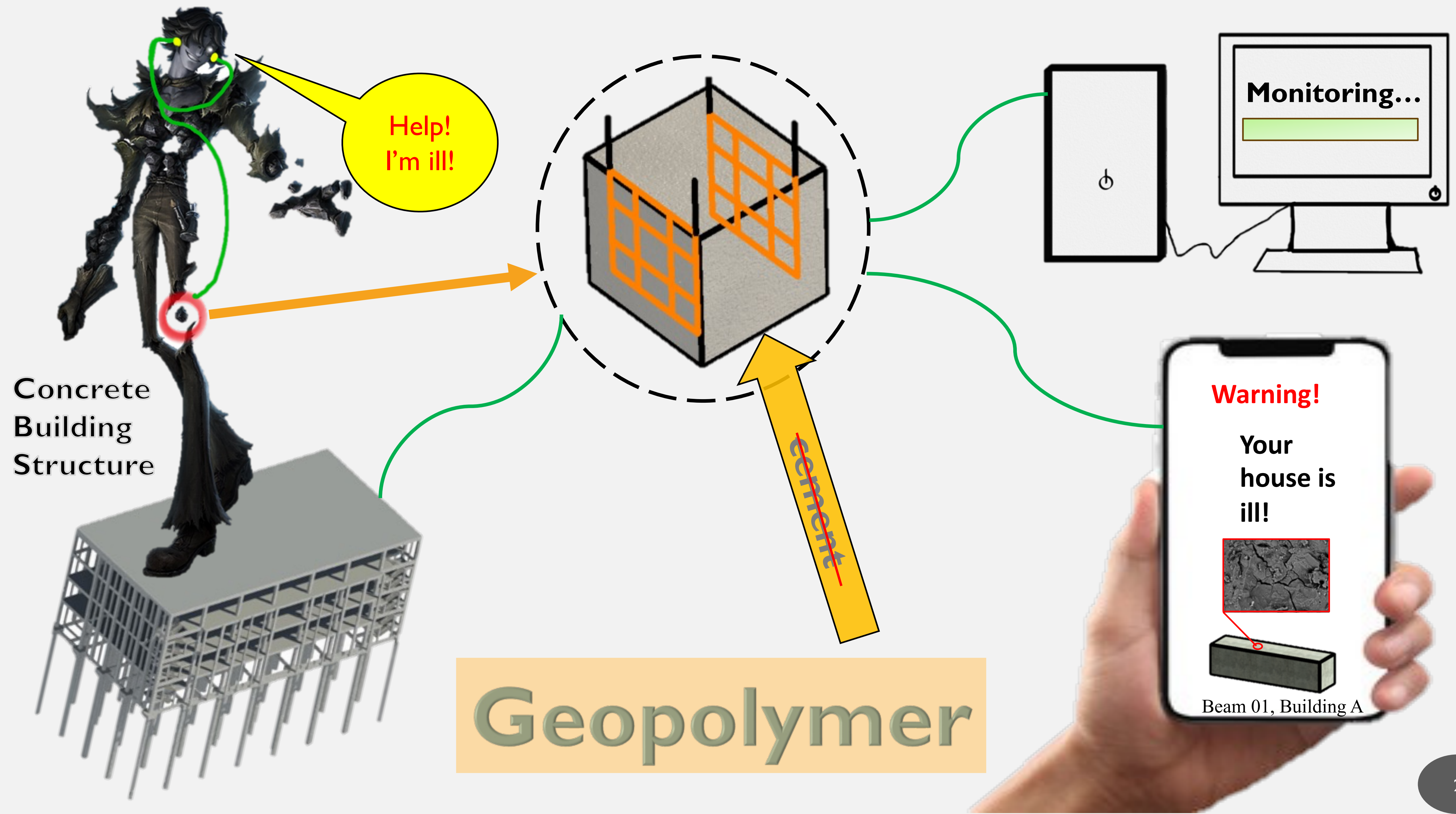
Help!
I'm ill!
Concrete
Building
Structure
~~cement~~
Geopolymer
Monitoring...
Warning!
Your
house is
ill!
Beam 01, Building A

Piezoresistive behaviour

Stress/strain → Electricity

Resistance-based

- Electrical resistivity (R)
- piezoresistivity effect

$$R=\rho L/S$$

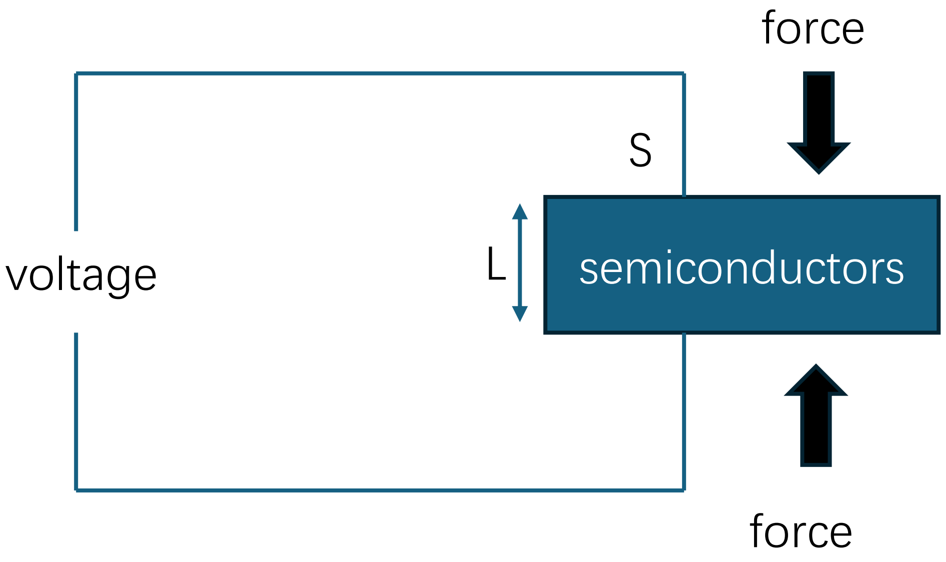

geometry change + conductivity (ρ) change

Capacitance-based

- Electrical capacitance(C) (storage of electric charge (Q)) and/or electric field (E)
- direct piezoelectric effect

$$C = \varepsilon * A / d$$

$$E=U/d$$

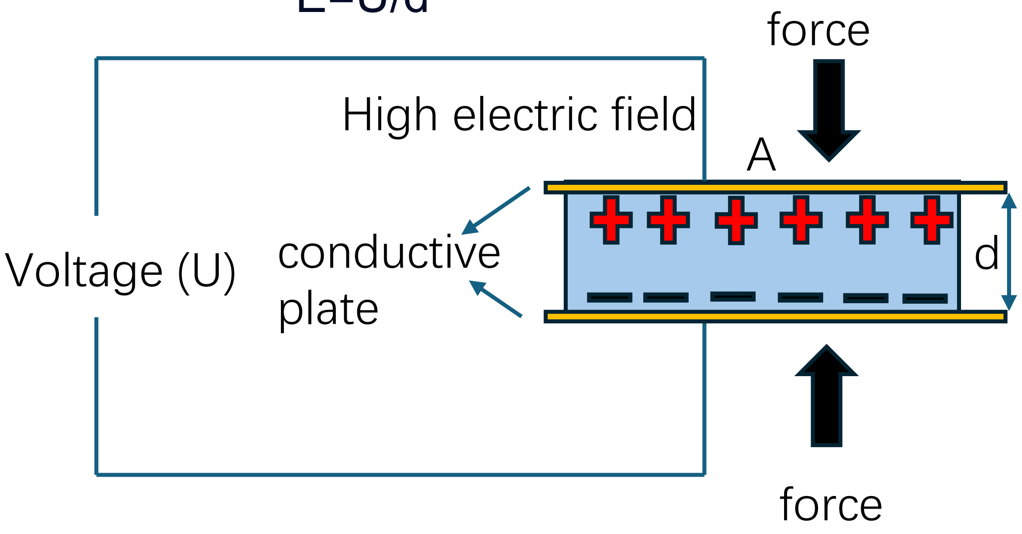

geometry change + permittivity (ε) change

What is self-sensing materials?

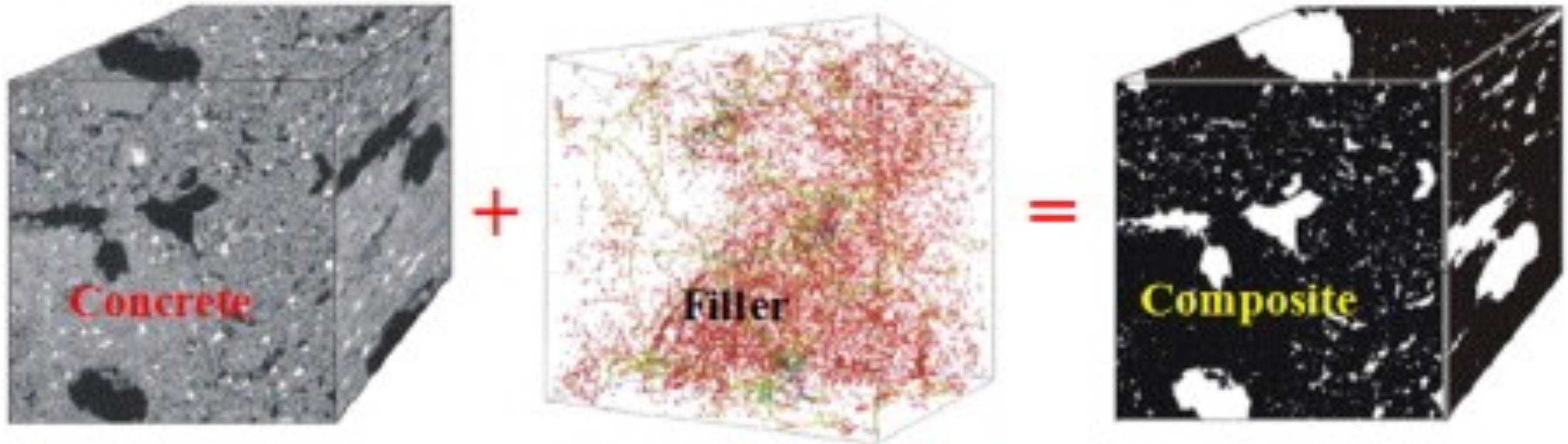

Structure of self-sensing concrete (Han et al. 2014b)

Non-conductive matrix

Cement-based
AAMs
Geopolymer

Concrete
Mortar
Paste

Conductive functional fillers

Carbon/silica-based
Metal-based

Particles
Fibres

Semi-conductive sensor

Self-sensing materials

MATRIX

MATERIALS
FRESH AND HARDENED PROPERTIES

Raw materials

Na_2SiO_3

Fly ash

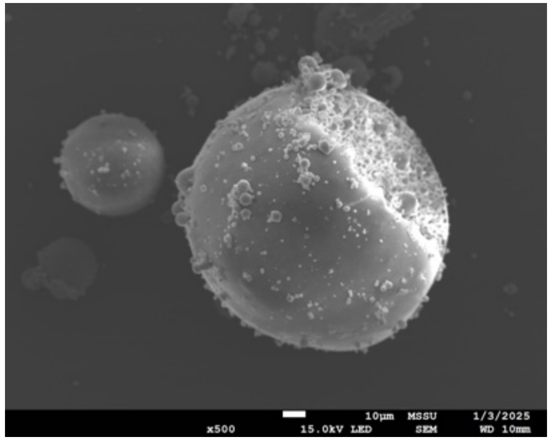

GGBS

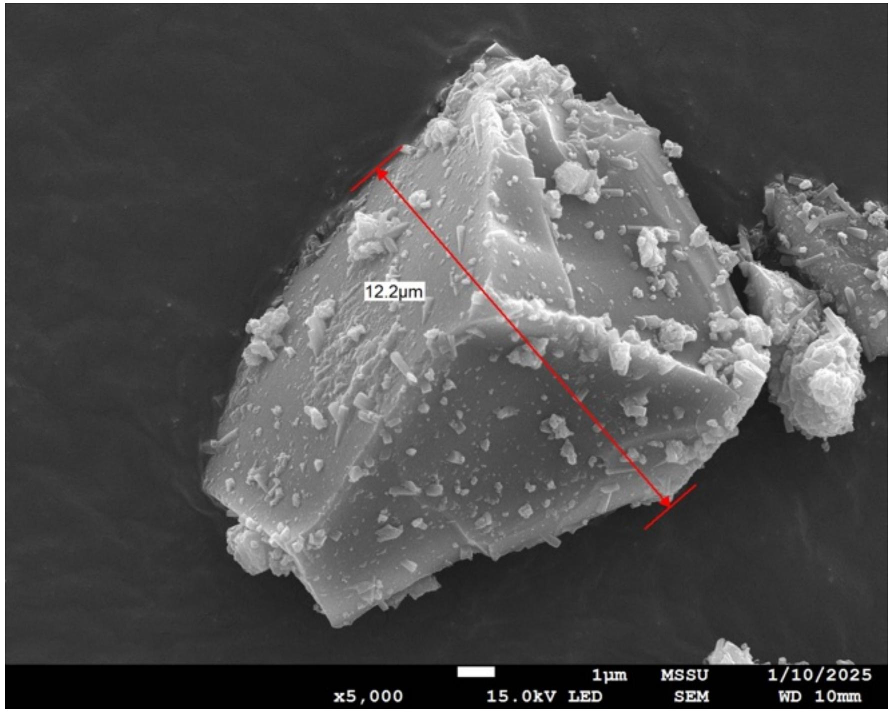

Sand (<5mm)

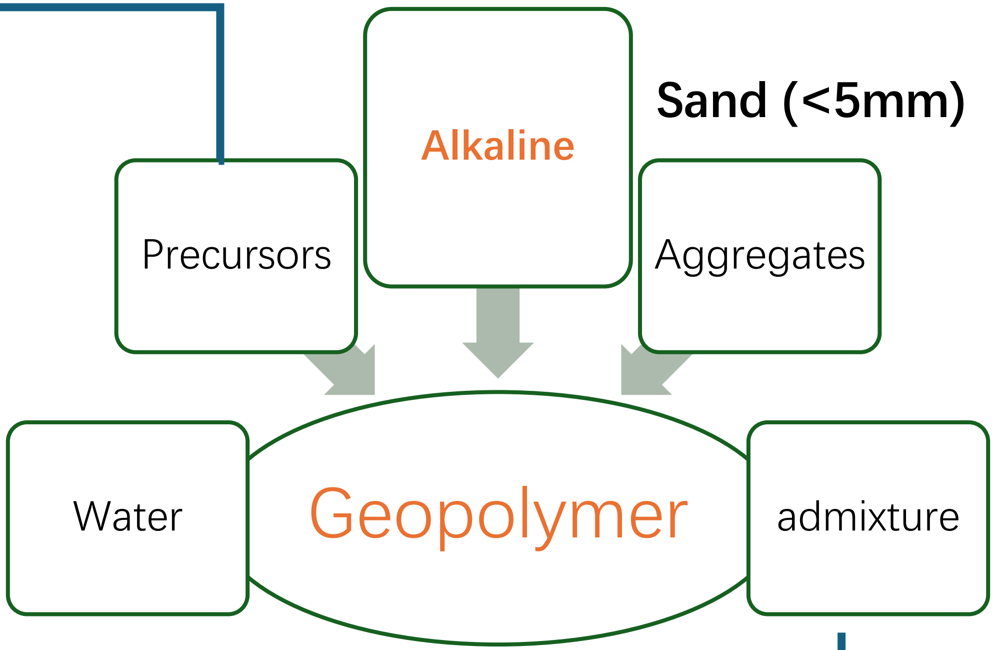

Superplasticizer

(Sika)

Raw materials

Fly ash (class F)

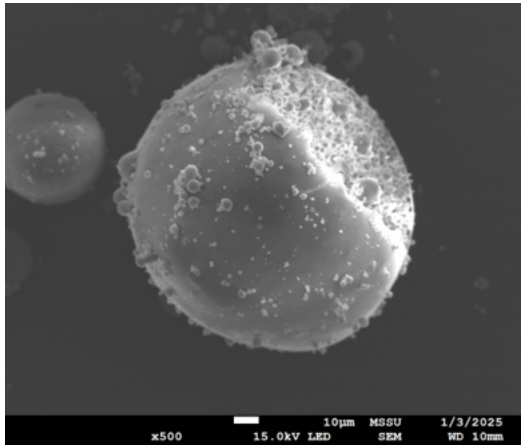

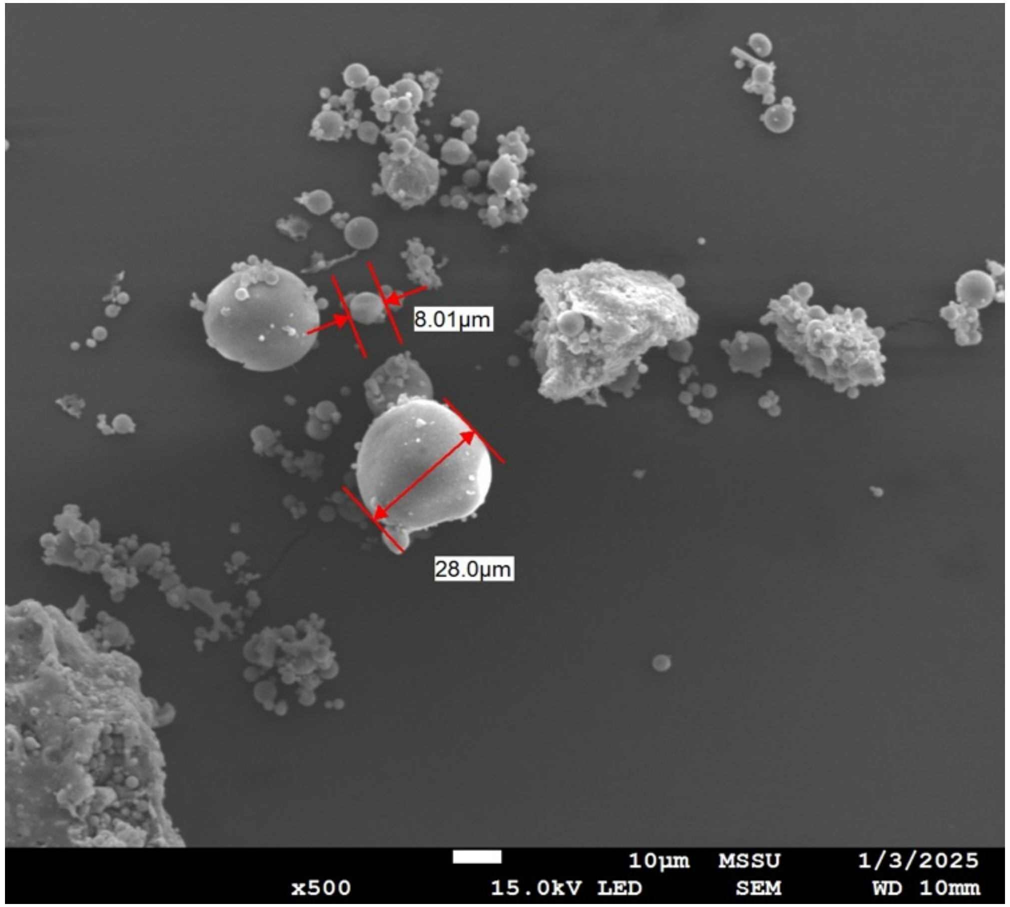

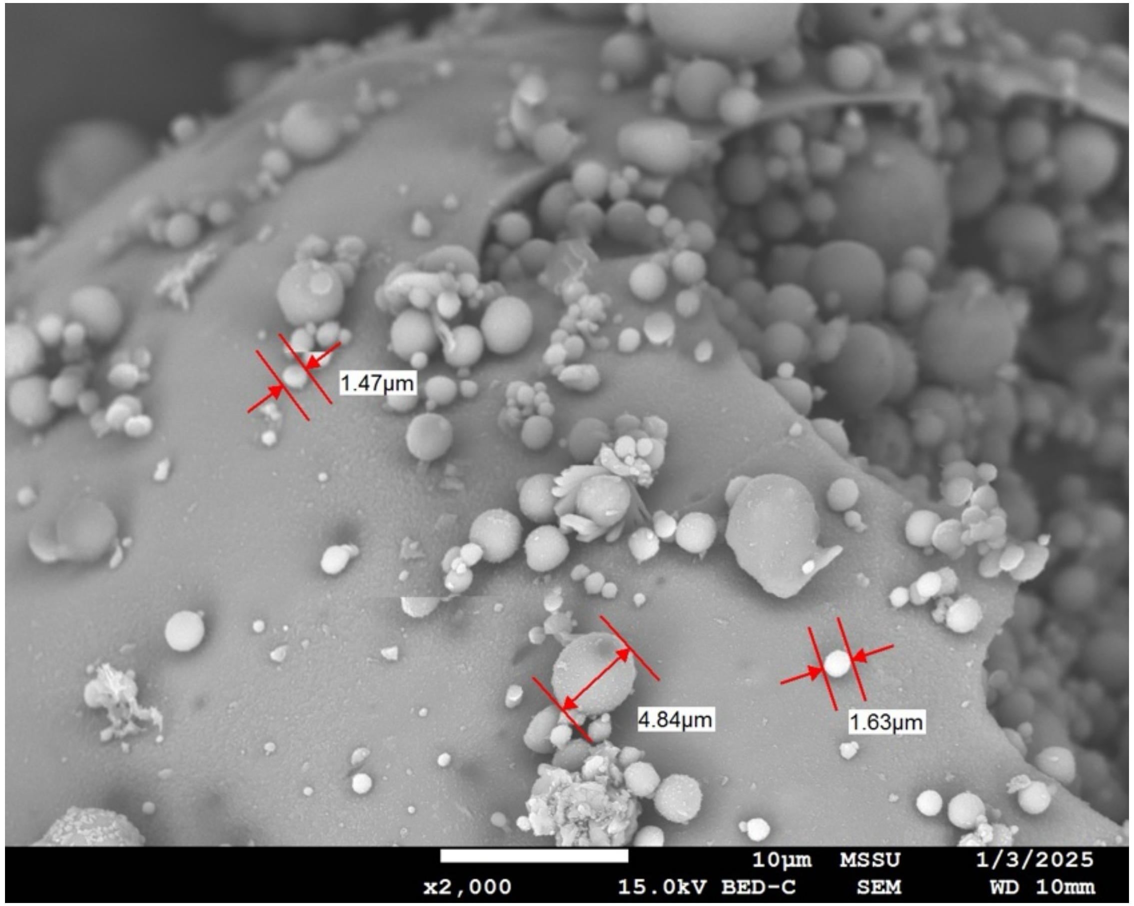

Trial mixes

Mix design

1

- Free water/binder ratio (w/b): 0.35 Superplasticiser (SP)/binder ratio: 0.5%
- The moisture content of Sand: 6% Assumed Na_2SiO_3 concentration: 6M

2

Three parameters:

FA/GGBS: fly ash/GGBS ratio

A/B: **activator/binder ratio**

Binder content

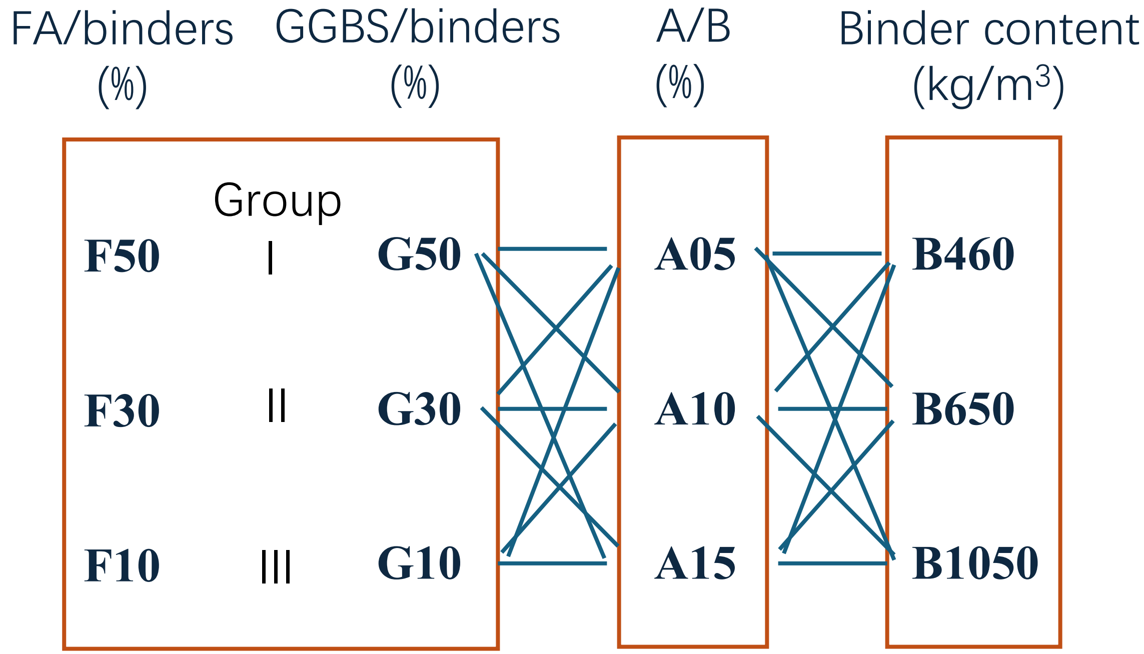

Mix ID - 27 mixes

Mix ID	FA	GGBS	Na_2SiO_3	Dry Sand	Total Water	SP
F50G50A15B460	230	230	69	1593	263	2.30
F50G50A10B460	230	230	46	1593	263	2.30
F50G50A05B460	230	230	23	1593	263	2.30
F50G50A15B650	325	325	98	1219	306	3.25
F50G50A10B650	325	325	65	1219	306	3.25
F50G50A05B650	325	325	33	1219	306	3.25
F50G50A15B1050	525	525	158	483	399	5.25
F50G50A10B1050	525	525	105	483	399	5.25
F50G50A05B1050	525	525	53	483	399	5.25

Group I mix design (in kg/m³) (Zhang et al. 2024)

Mix samples

Room temperature curing

Fresh | **7 days** | **28 days** | **84 days**

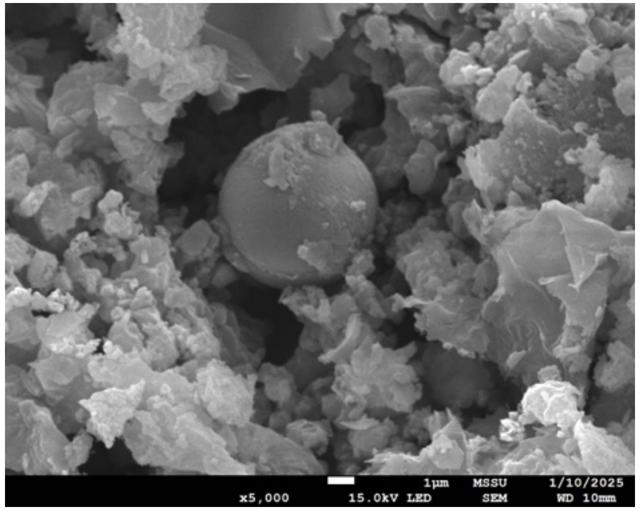

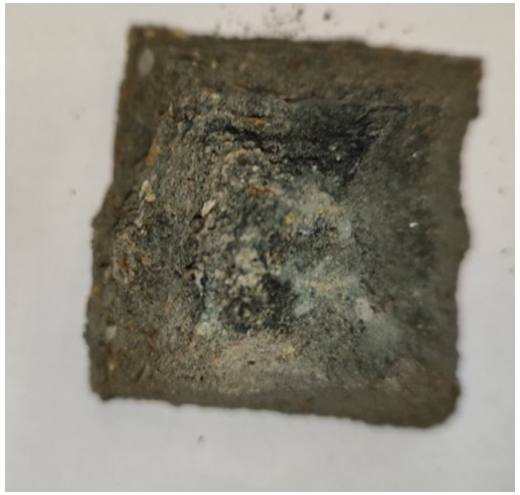

Flowability

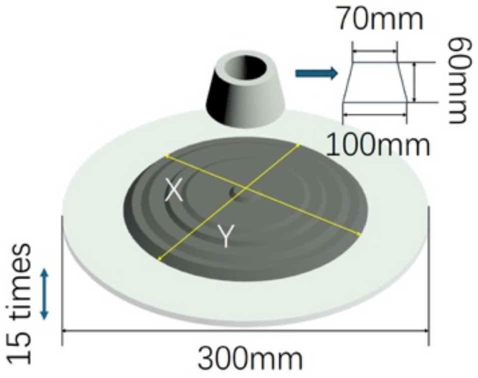

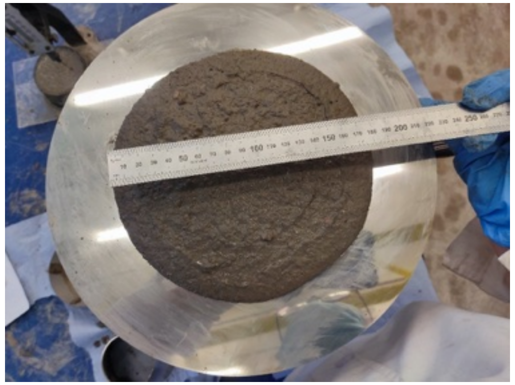

Flow table test

- Mixes with lower A/B, FA/GGBS and binder content led to a smaller flow spread.
- The influence of binder content may be more significant than the binder proportion.

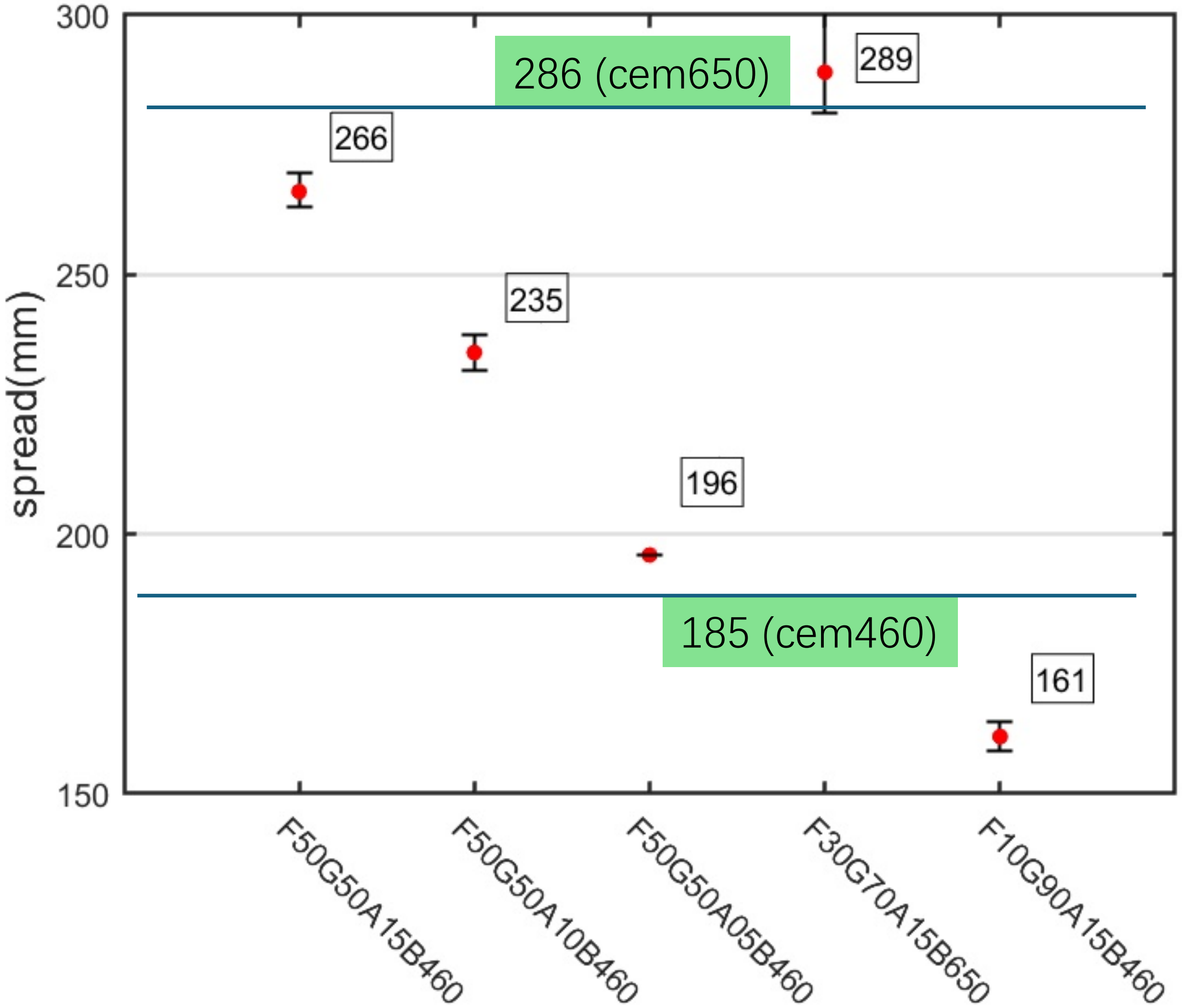

Flowability of matrix (in mm) (Zhang et al. 2024)

Compressive strength

41 MPa at 7d and over 55MPa (cem650)
31 MPa at 7d and over 40MPa (cem460)

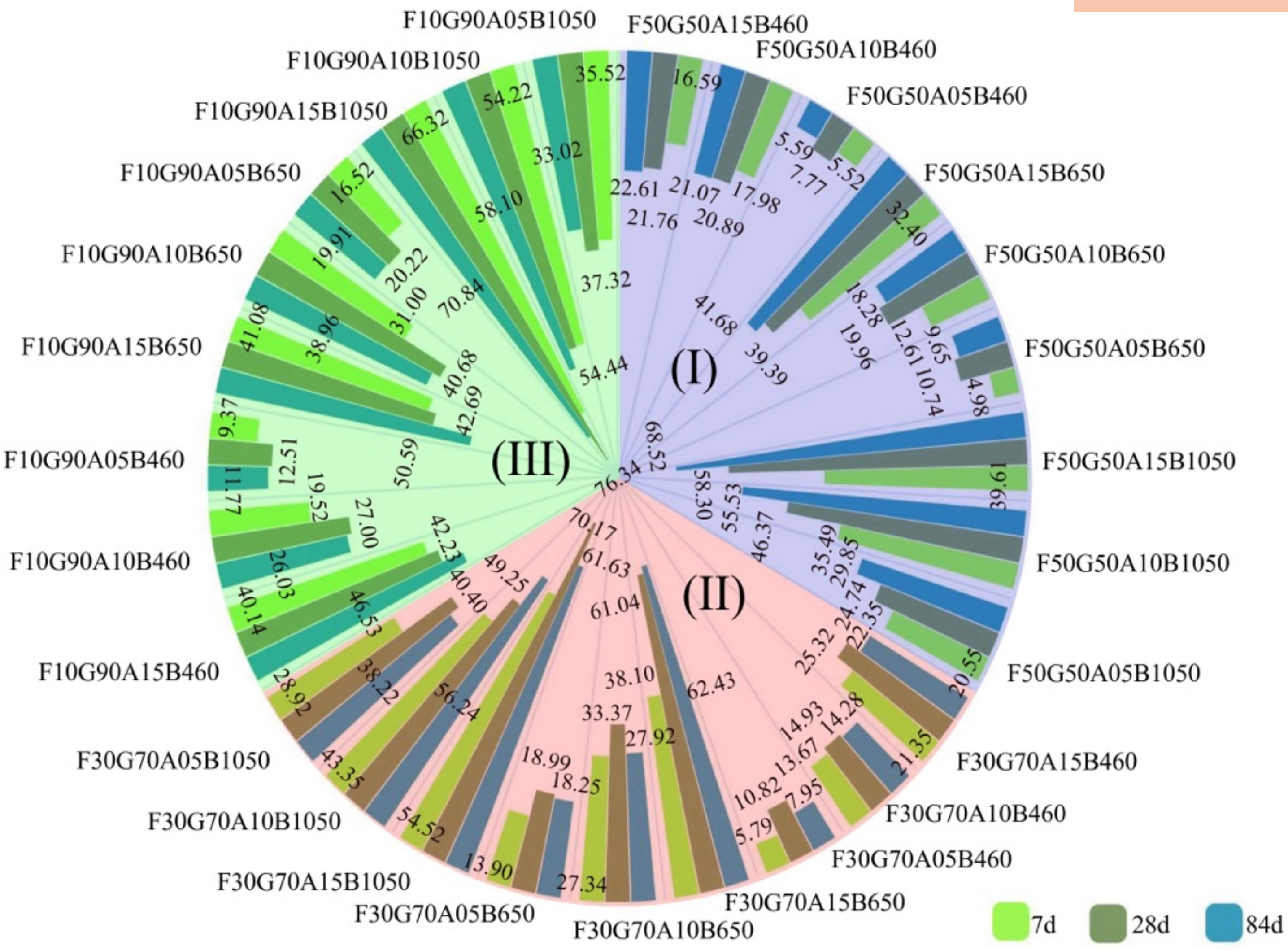

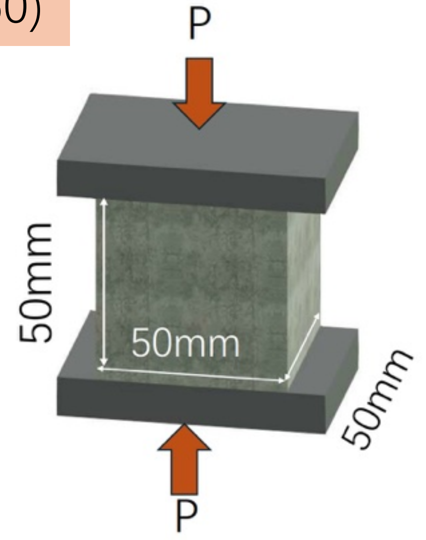

- The highest compressive strength reached over 65 MPa at 7 days, 28 days, and 84 days.
- Compressive strength increases caused by decreasing A/B and increasing binder content.
- Mixes with the lower FA/GGBS ratio had higher compressive strength when the binder content was high.

Compressive strength of matrix (in MPa) (Zhang et al. 2024)

Flexural strength

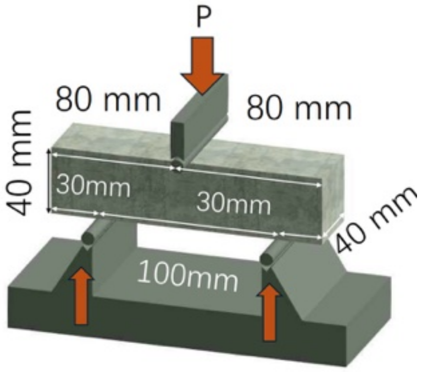

- The 28-day flexural strength of the 27 mixes varied from 1.64 MPa to 5.86 MPa.
- Strength tended to increase with decreasing FA/GGBS and increasing A/B ratios.

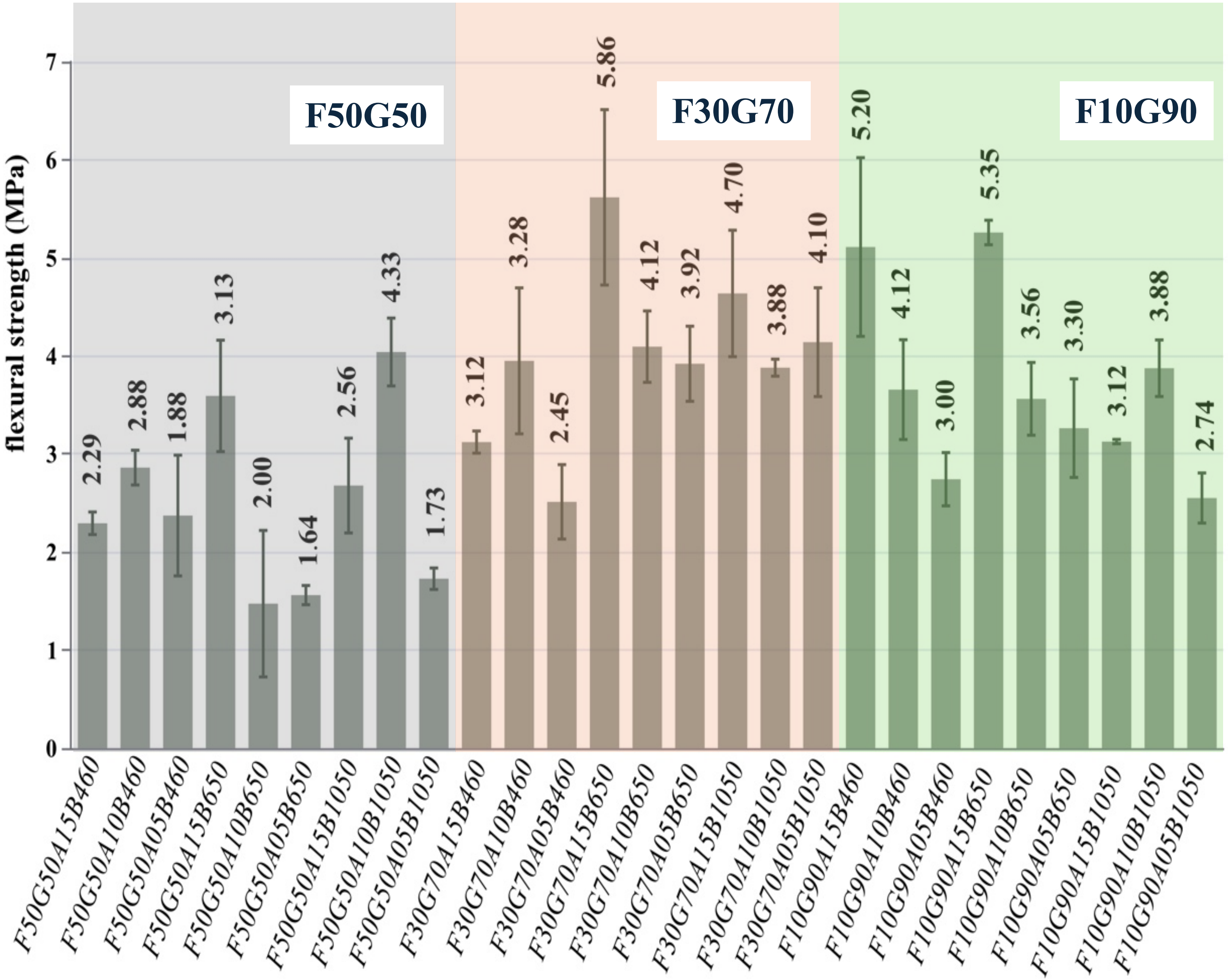

Flexural strength of matrix (in MPa) (Zhang et al. 2024)

Embodied carbon emissions

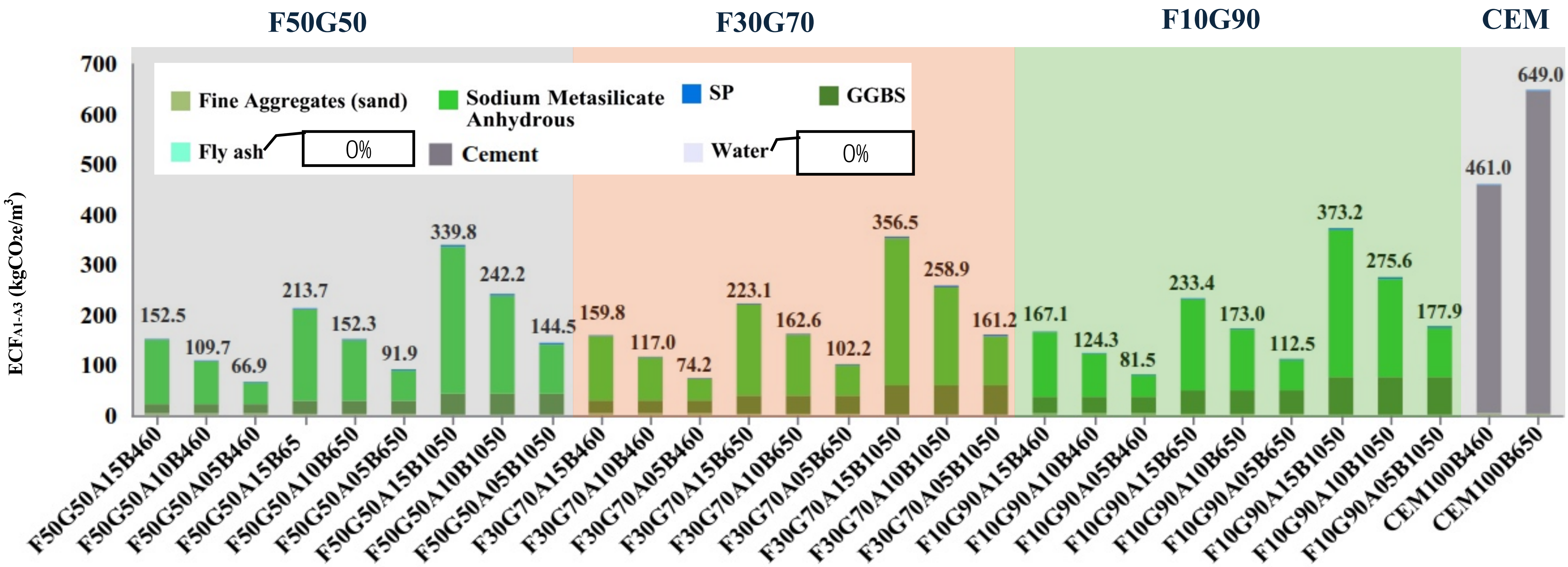

Materials	Sand	Na_2SiO_3	GGBS	FA	SP	Water	Cement
Carbon emissions (A1-A3) ($kgCO_2eq/ton$)	2.6	1860	79.6	0.1	720	0	*860*

- 27 mixes had much lower carbon emissions compared to cement mortar.

Embodied carbon emissions (A1-A3) of matrix (Zhang et al. 2024)

WITH FUNCTIONAL FILLERS

MATERIALS
FRESH AND HARDENED PROPERTIES

Main types of conductive fillers

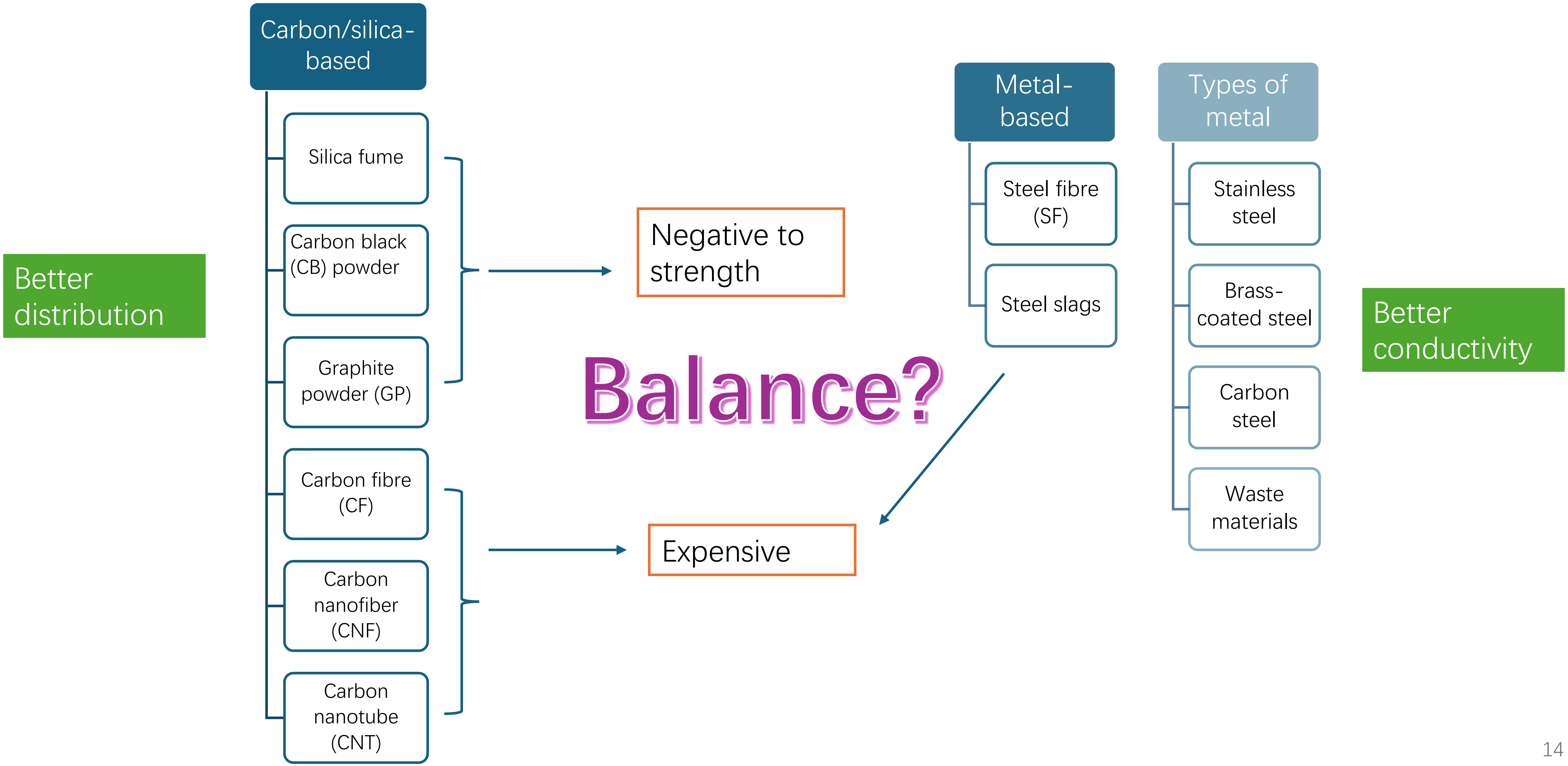

Graphite

F30G70A15B650 (M13) + graphite (5-10% by mass)

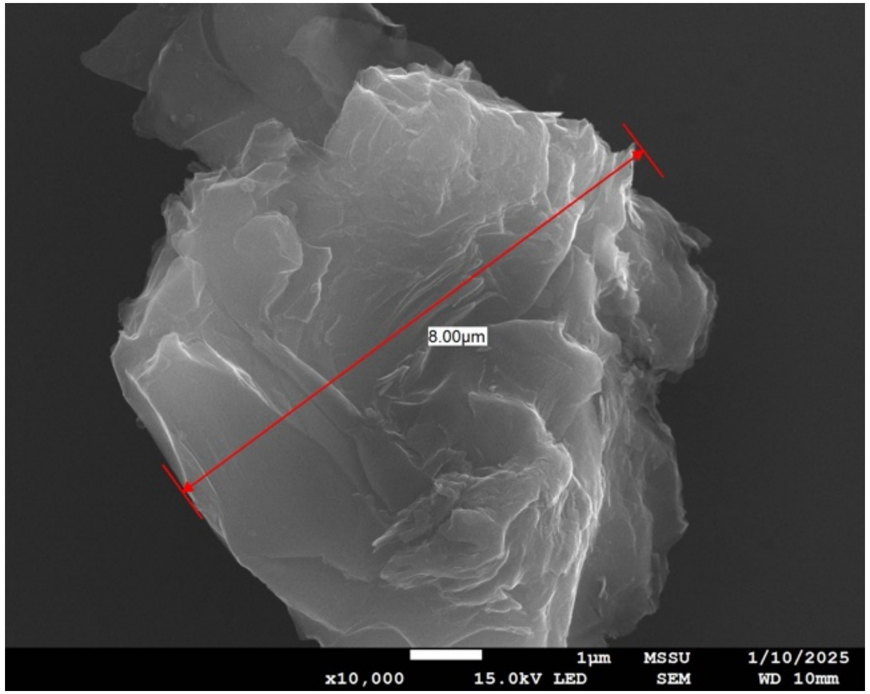

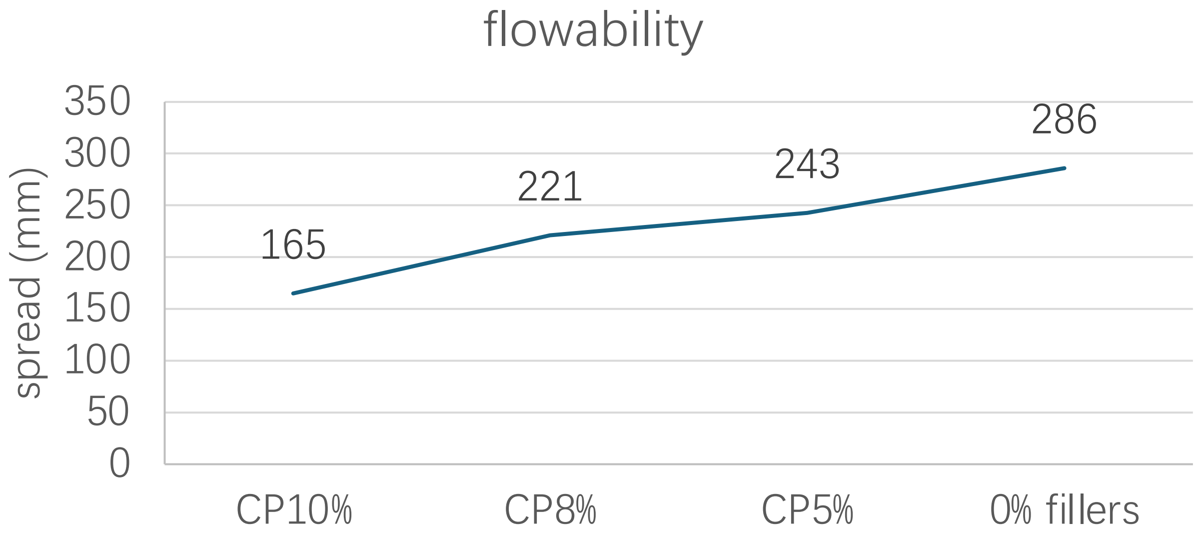

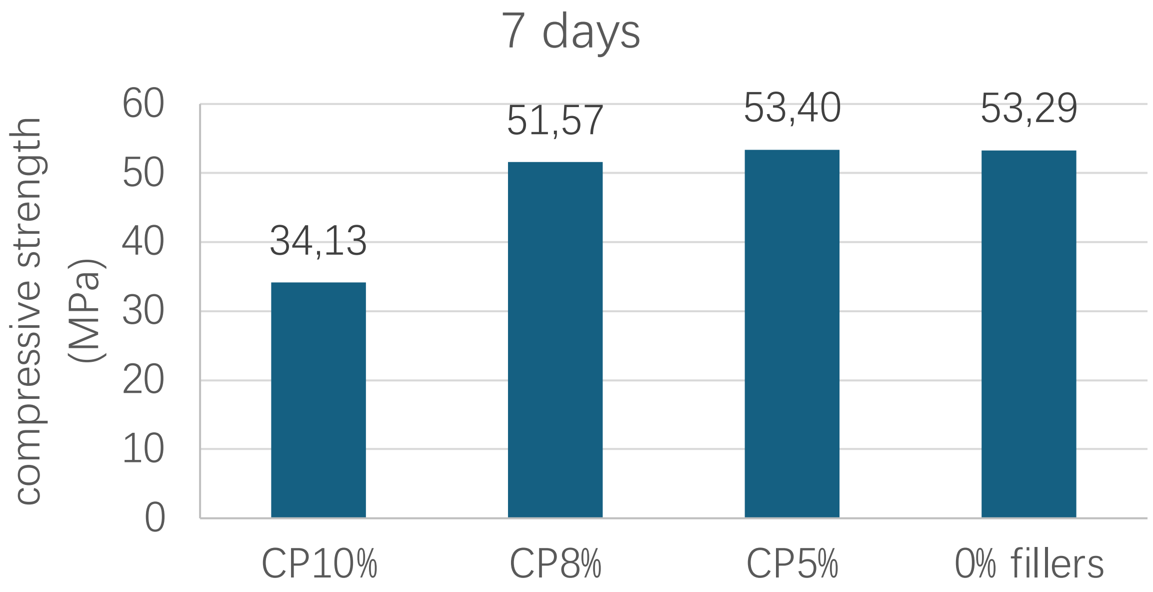

Steel fibres F30G70A15B650 (M13) + SF (0.5-5% by volume)

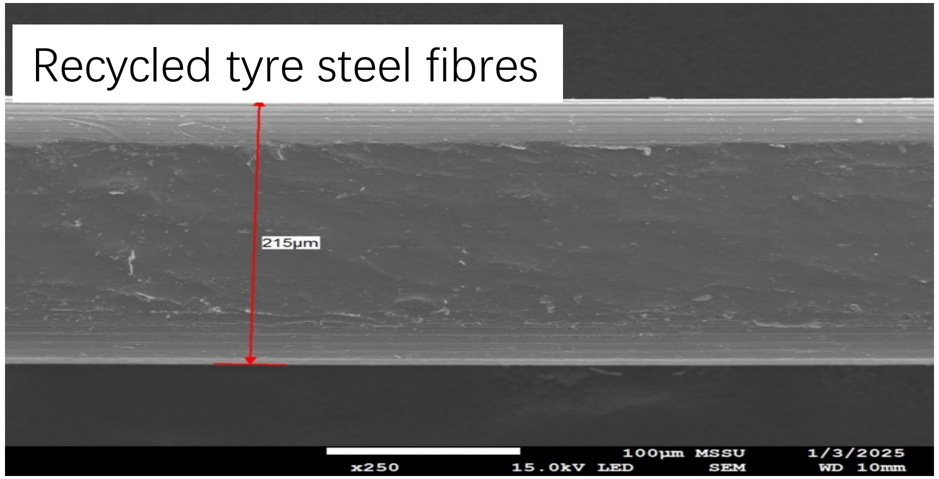

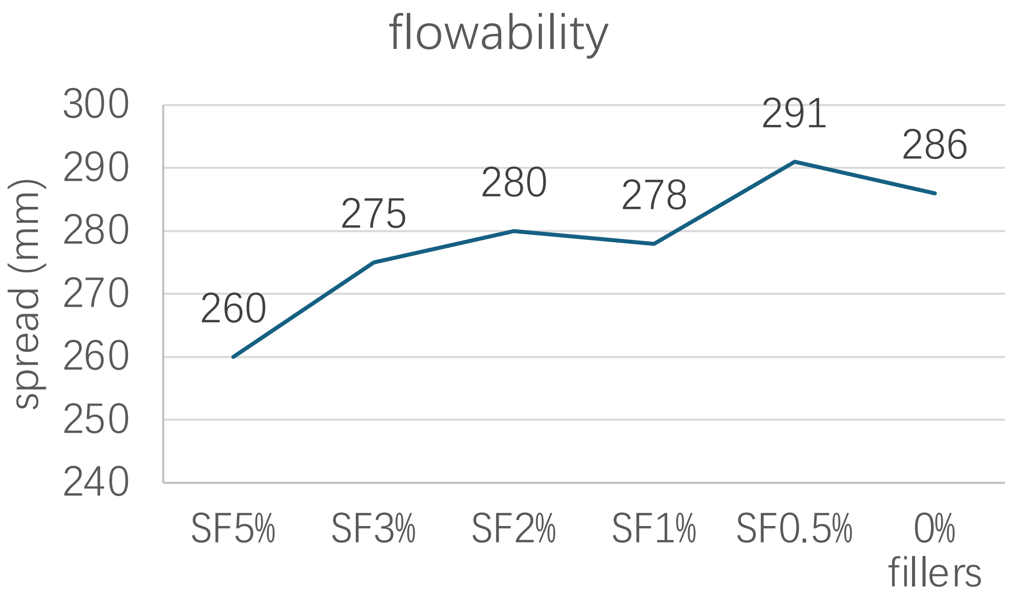

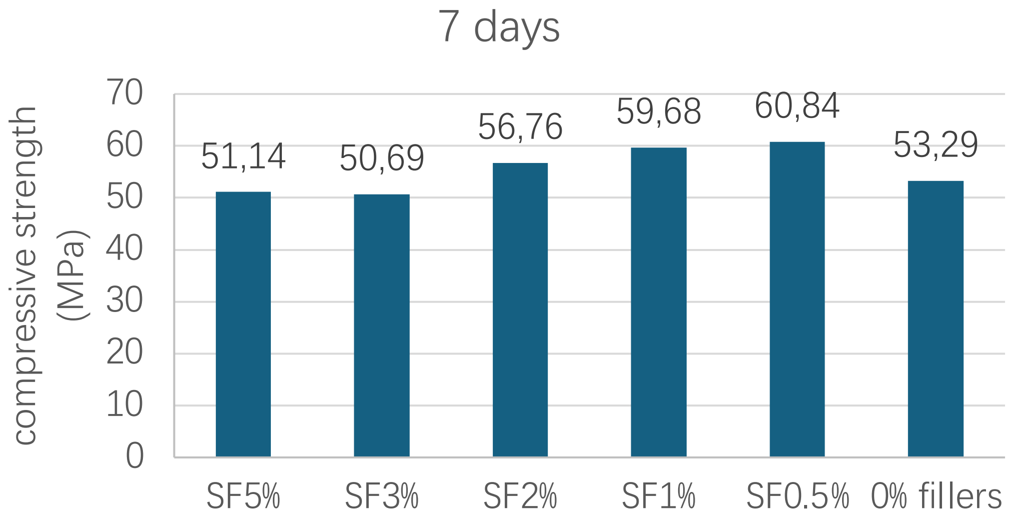

SELF-SENSING PERFORMANCE

Application of self-sensing materials

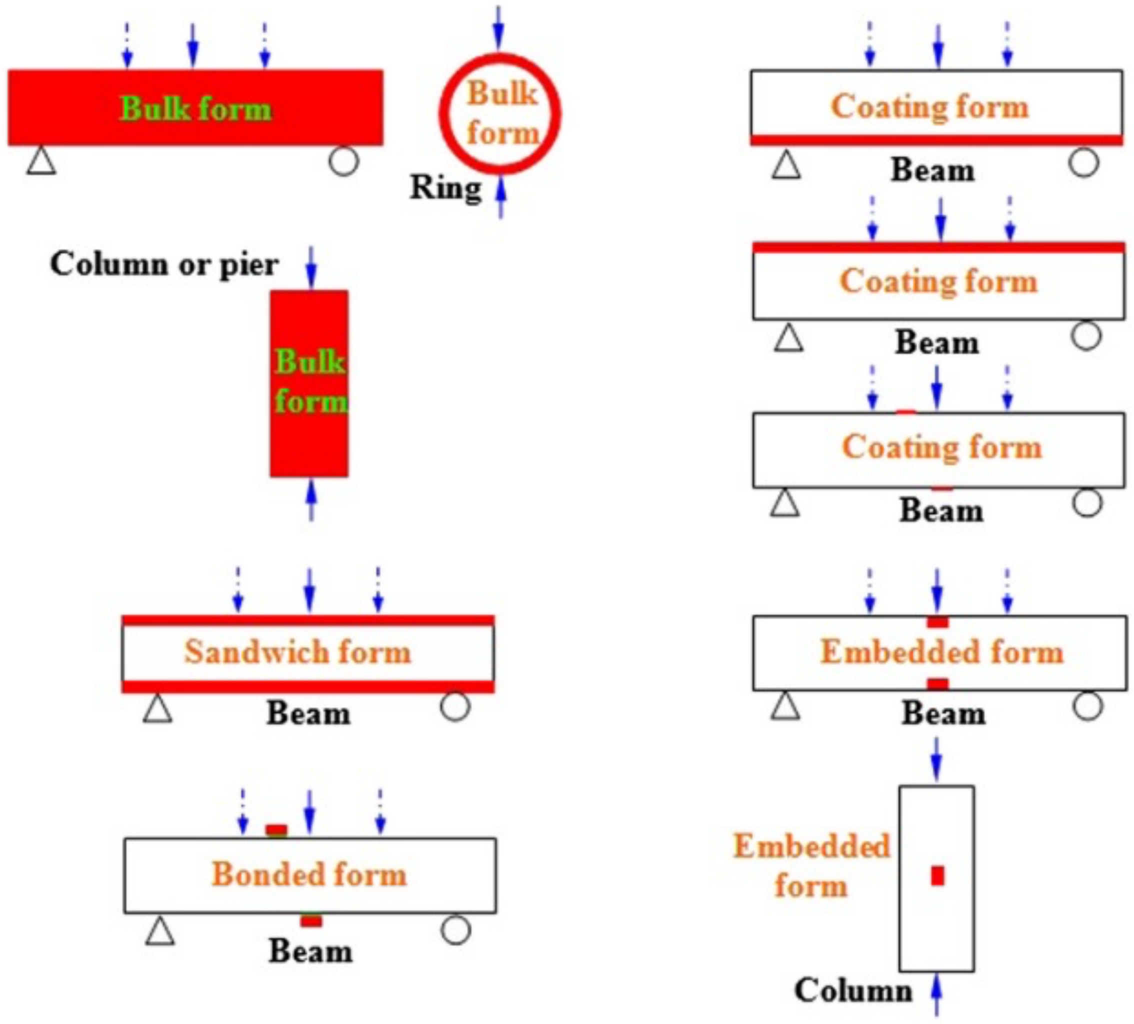

Typical application forms of self-sensing concrete for structural health monitoring (parts in red represent self-sensing concrete). (Han et al. 2014a)

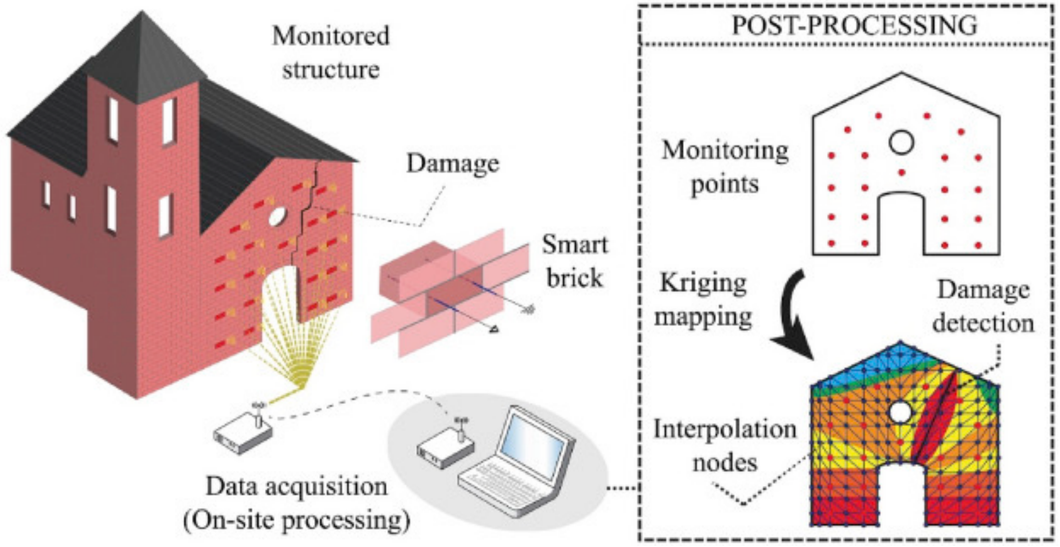

Schematic of smart bricks for masonry structures health monitoring (García-Macías and Ubertini 2019)

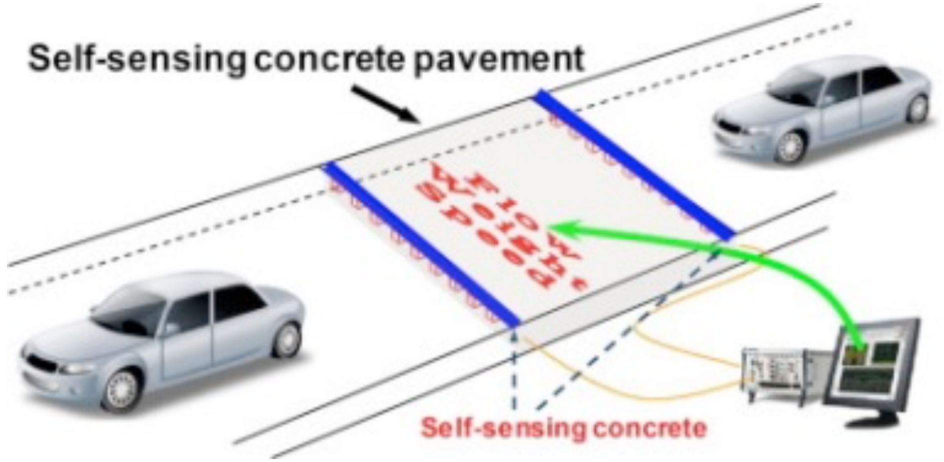

Schematic diagram of a self-sensing pavement structure for vehicle detection (Han et al. 2015)

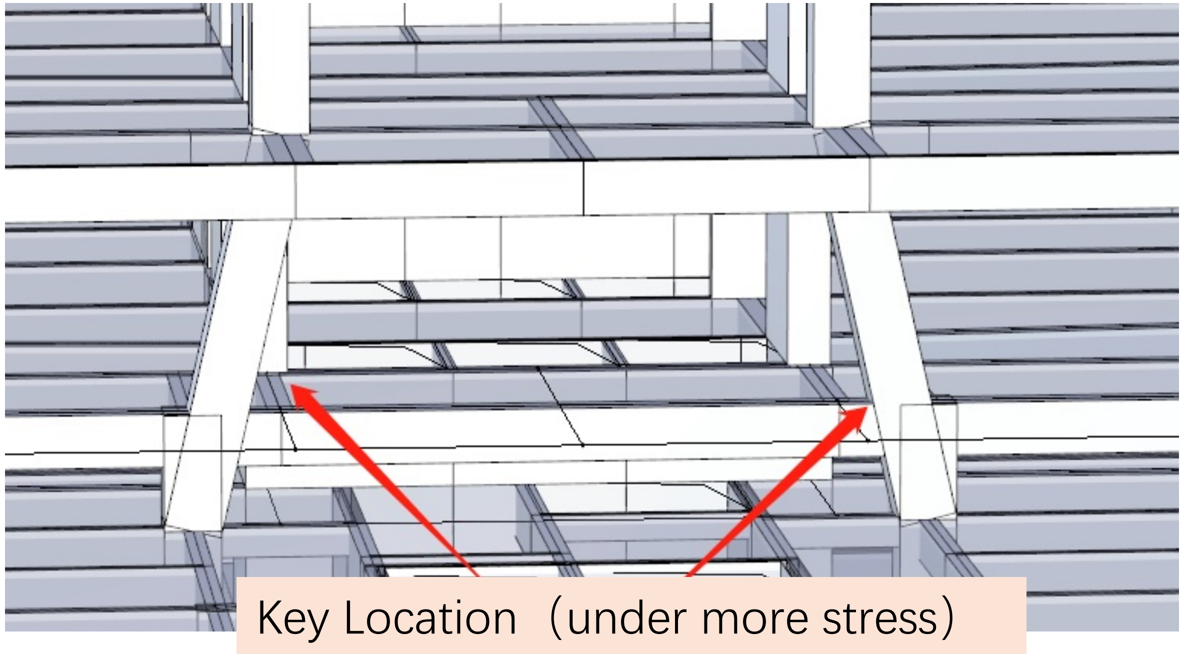

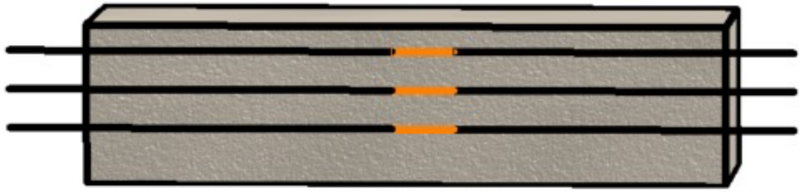

Cracks due to the normal sensors

Stress

Components that are much easy to be broken

Types of resistance-based measurements

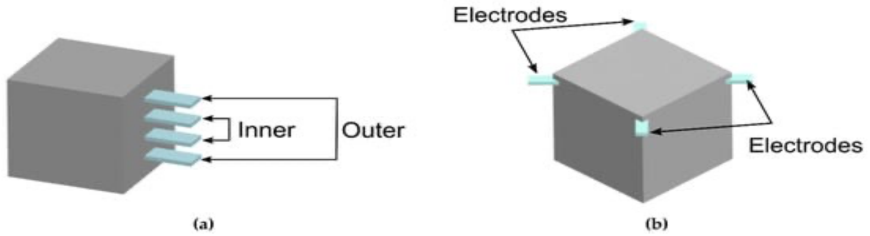

Electrode array for geopolymer sensing applications (**a**) serial arrangement (**b**) Van der Pauw arrangement (Vlachakis et al. 2020)

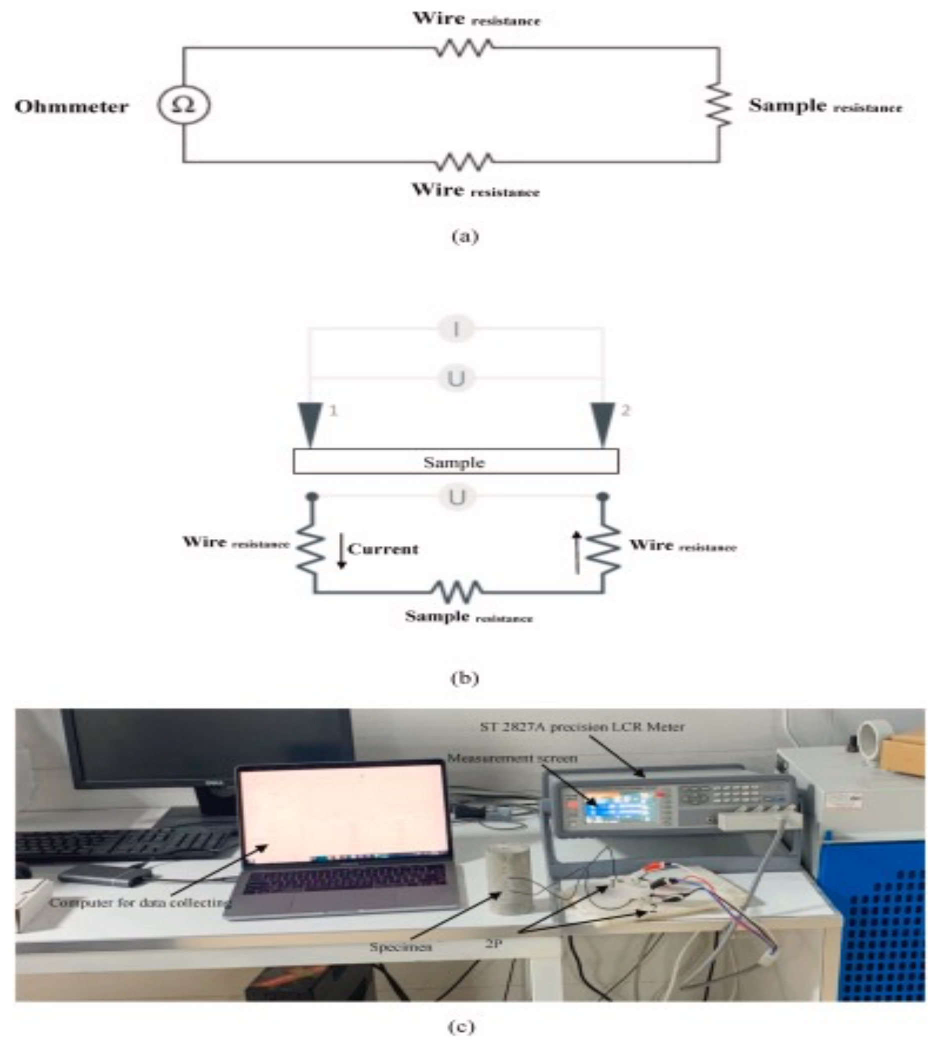

Two-probe (2P) method (Piro et al. 2023)

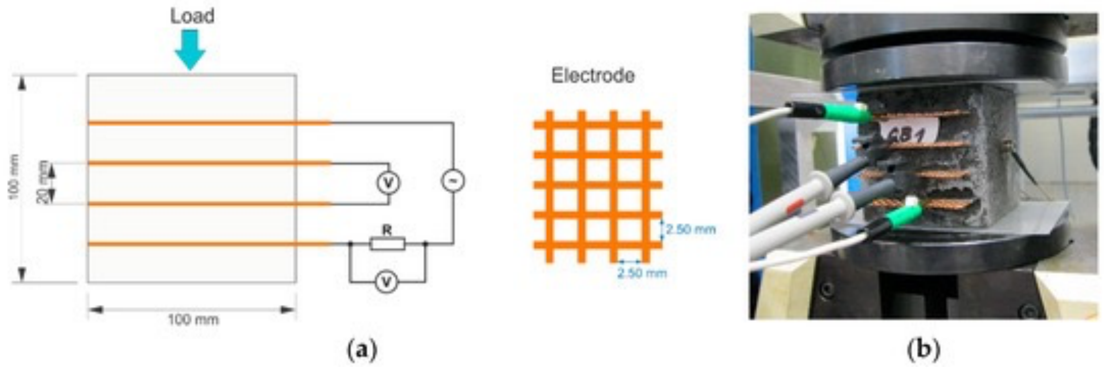

Four-probe for compression test of cube (Mizerová et al. 2021)

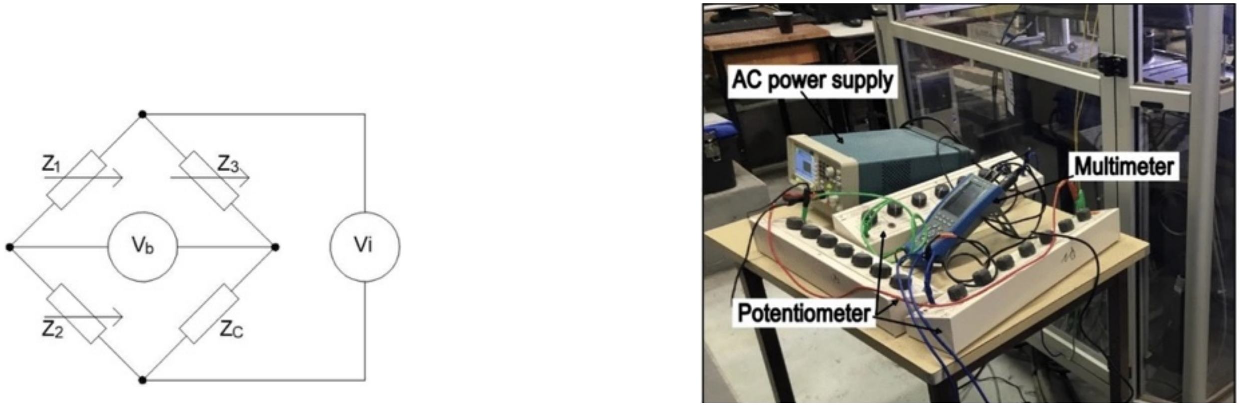

Layout of the AC Wheatstone bridge setup (Ferdiansyah et al. 2022; Shahzad et al. 2022)

Without conductive fillers-b3

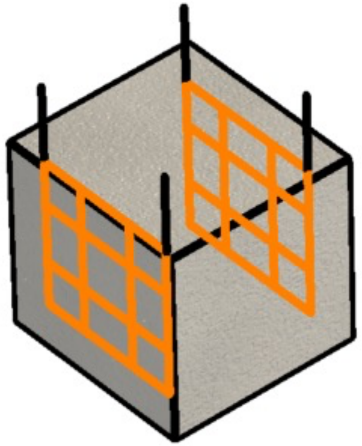

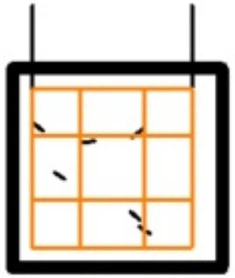

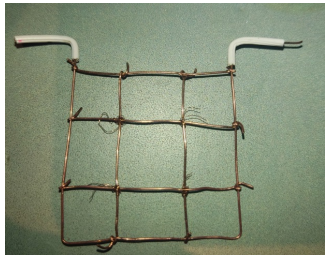

2-probe
4-wire

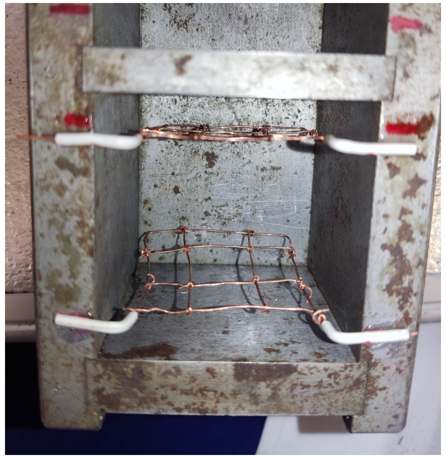

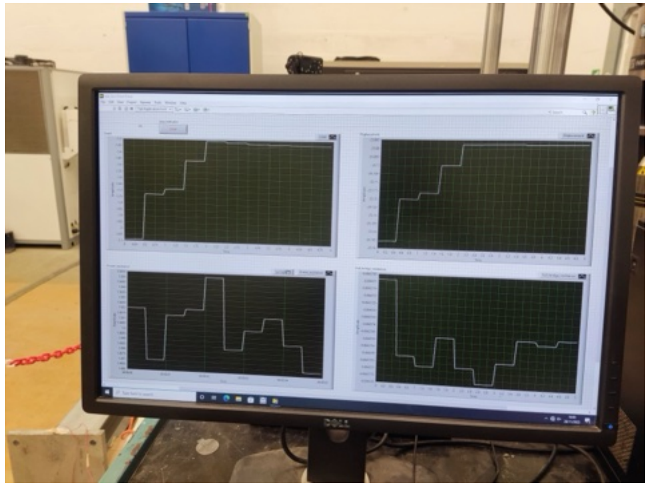

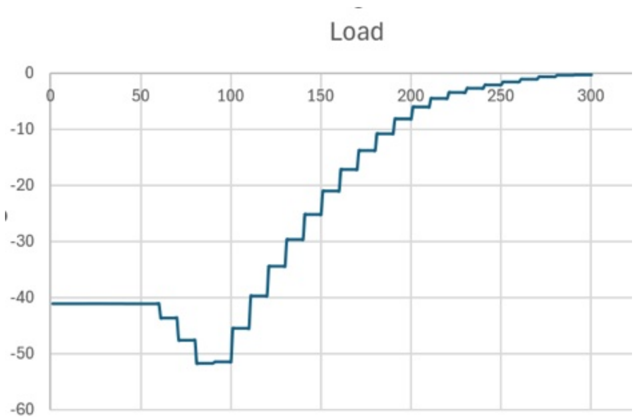

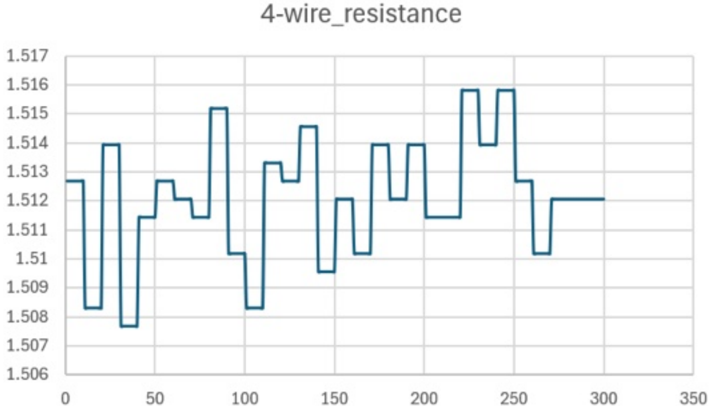

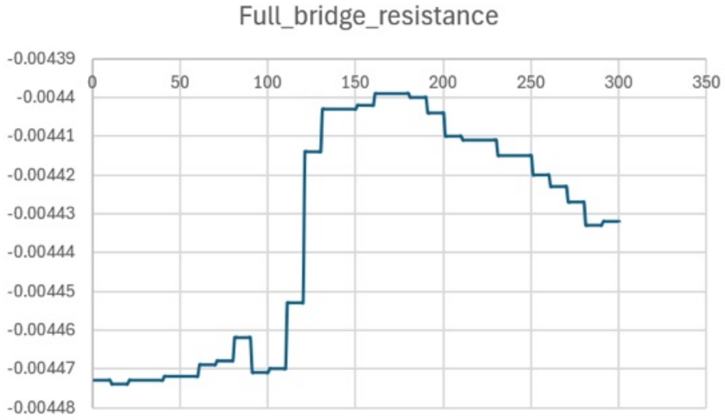

Without conductive fillers-b8

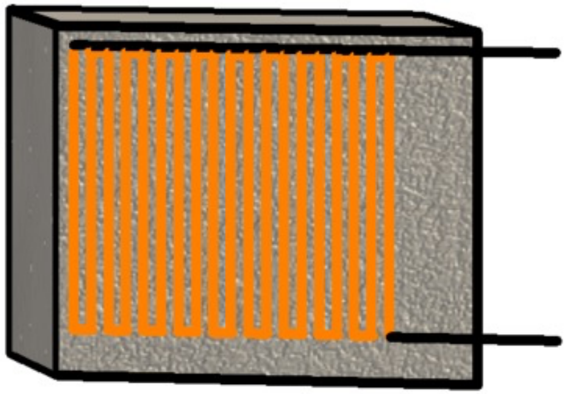

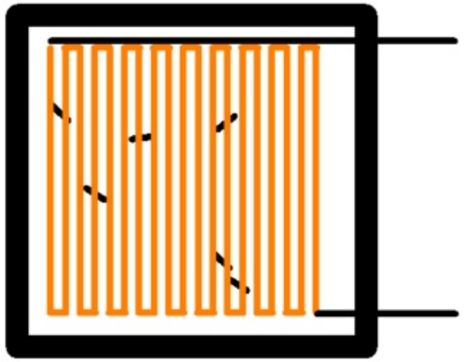

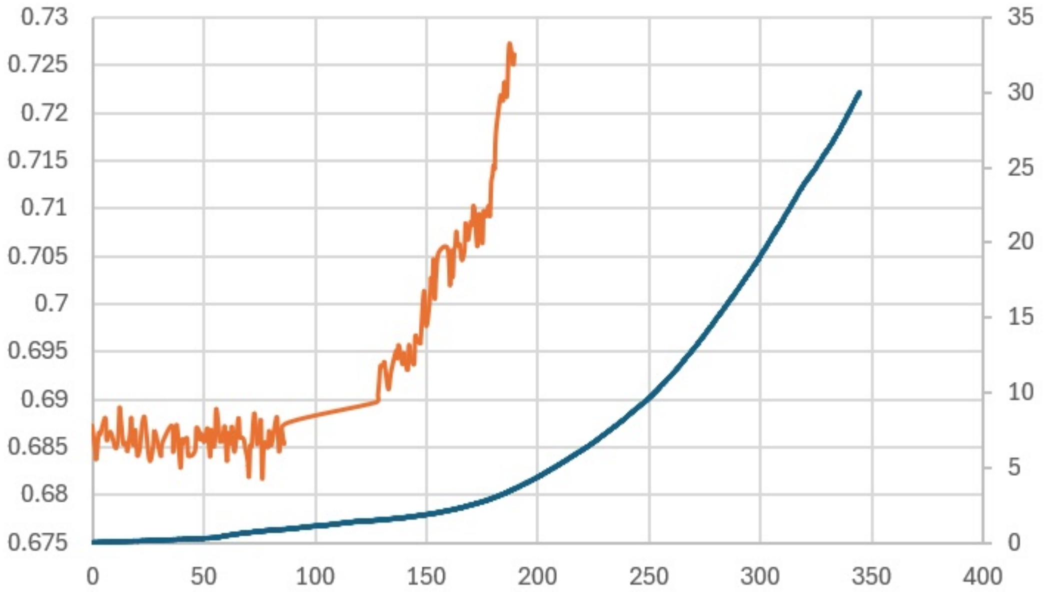

0.25

Zigzag instead of 19 wires

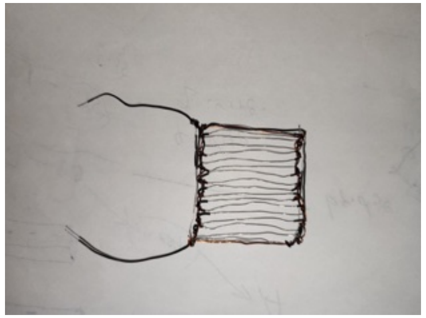

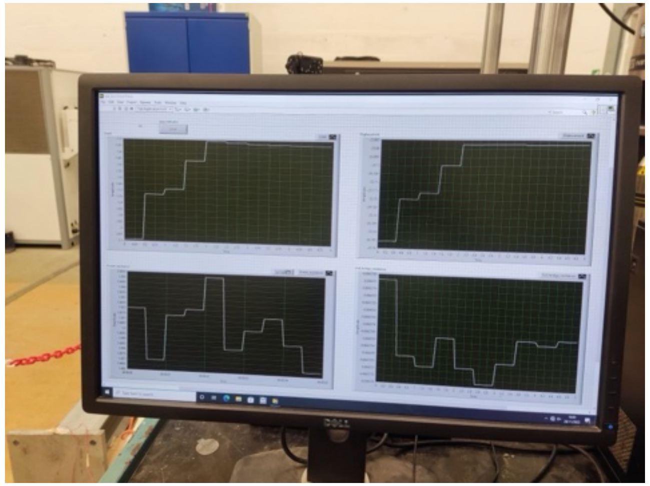

2-probe
4-wire

Self-sensing performance under cyclic loading

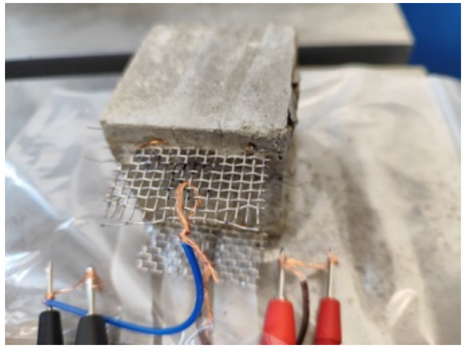

2-probe
2-wires
method with
DC

stress=Force/Area → Gauge factor=stress/FCR ← FCR=(R-Ro)/Ro

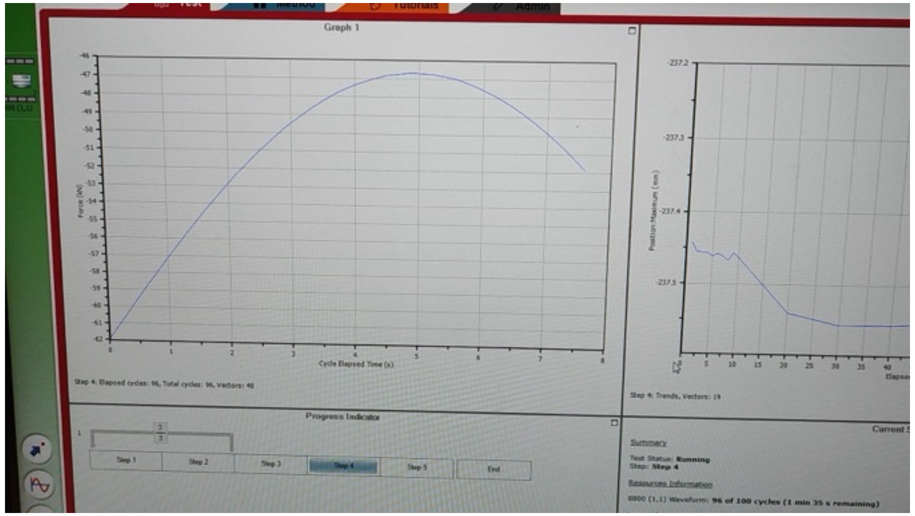

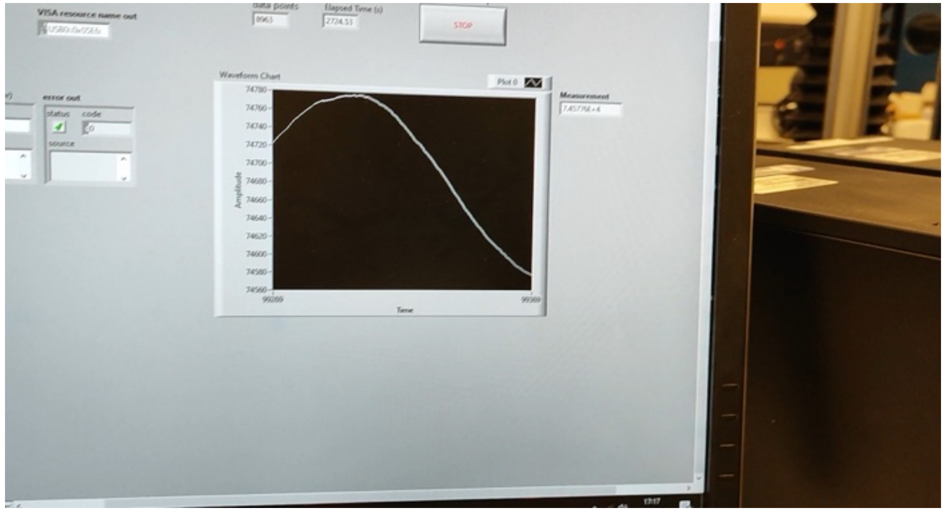

Force (kN)

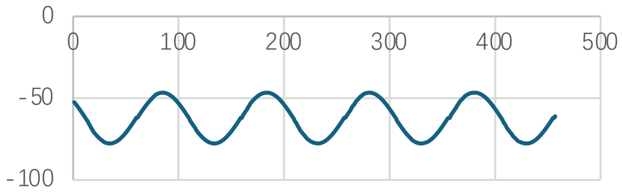

fractional change in electrical resistivity/resistance (FCR)

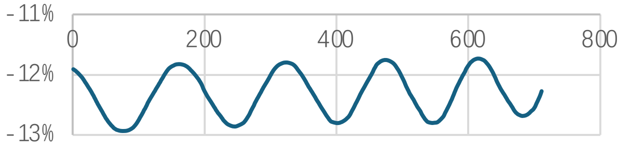

resistance

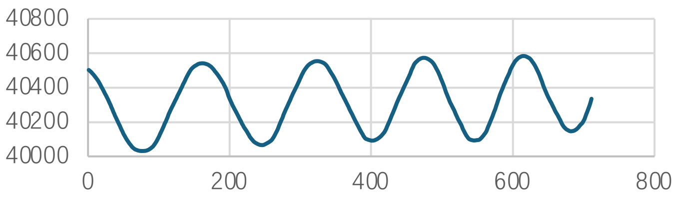

Self-sensing performance under cyclic loading

84days F50G50A15B650 (M4)

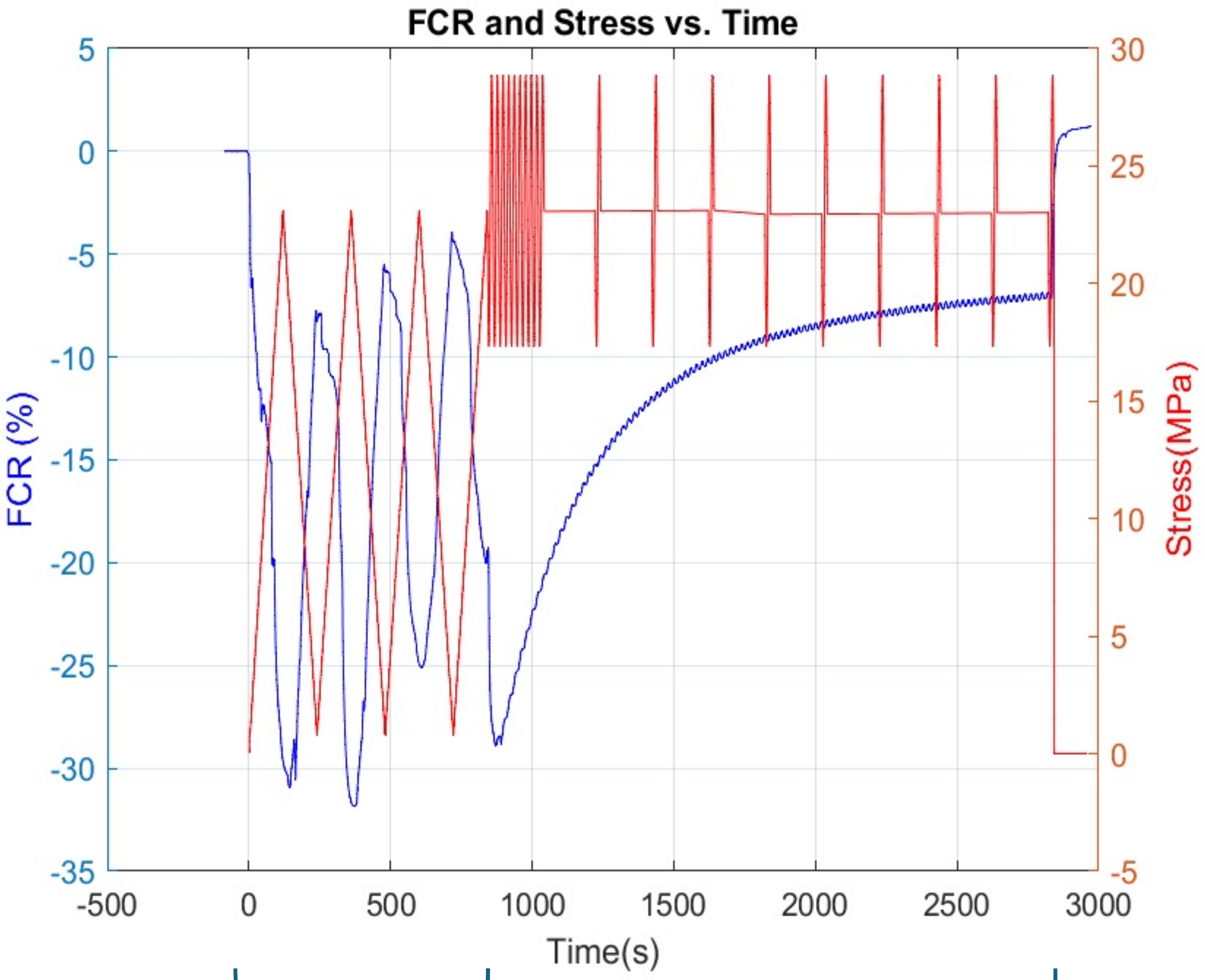

3 cycles
0.4 max loading

100 sin-shaped cycles
0.4-0.6 max loading

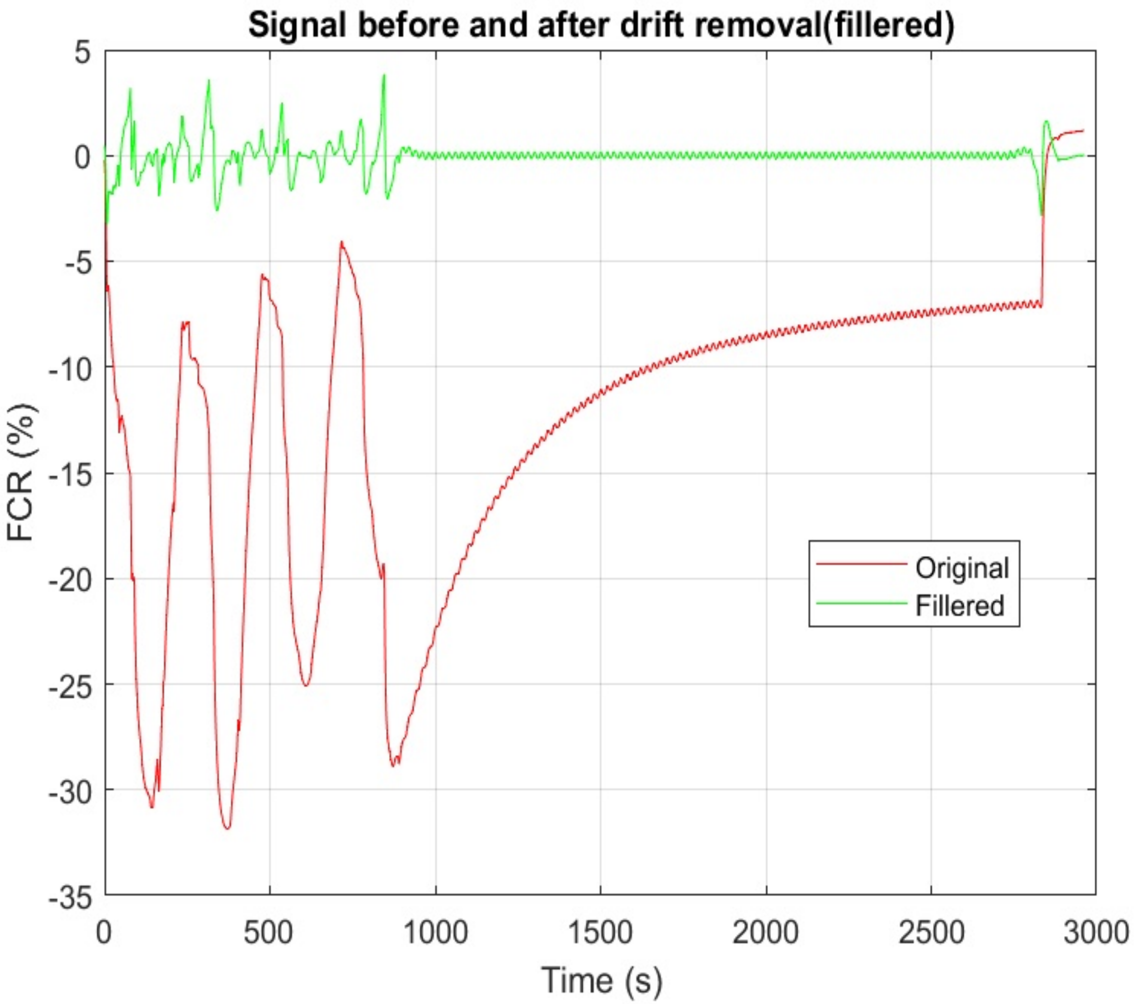

Signal drift ------electrical polarization

Geopolymer

Self-sensing performance under cyclic loading

84days CEM650

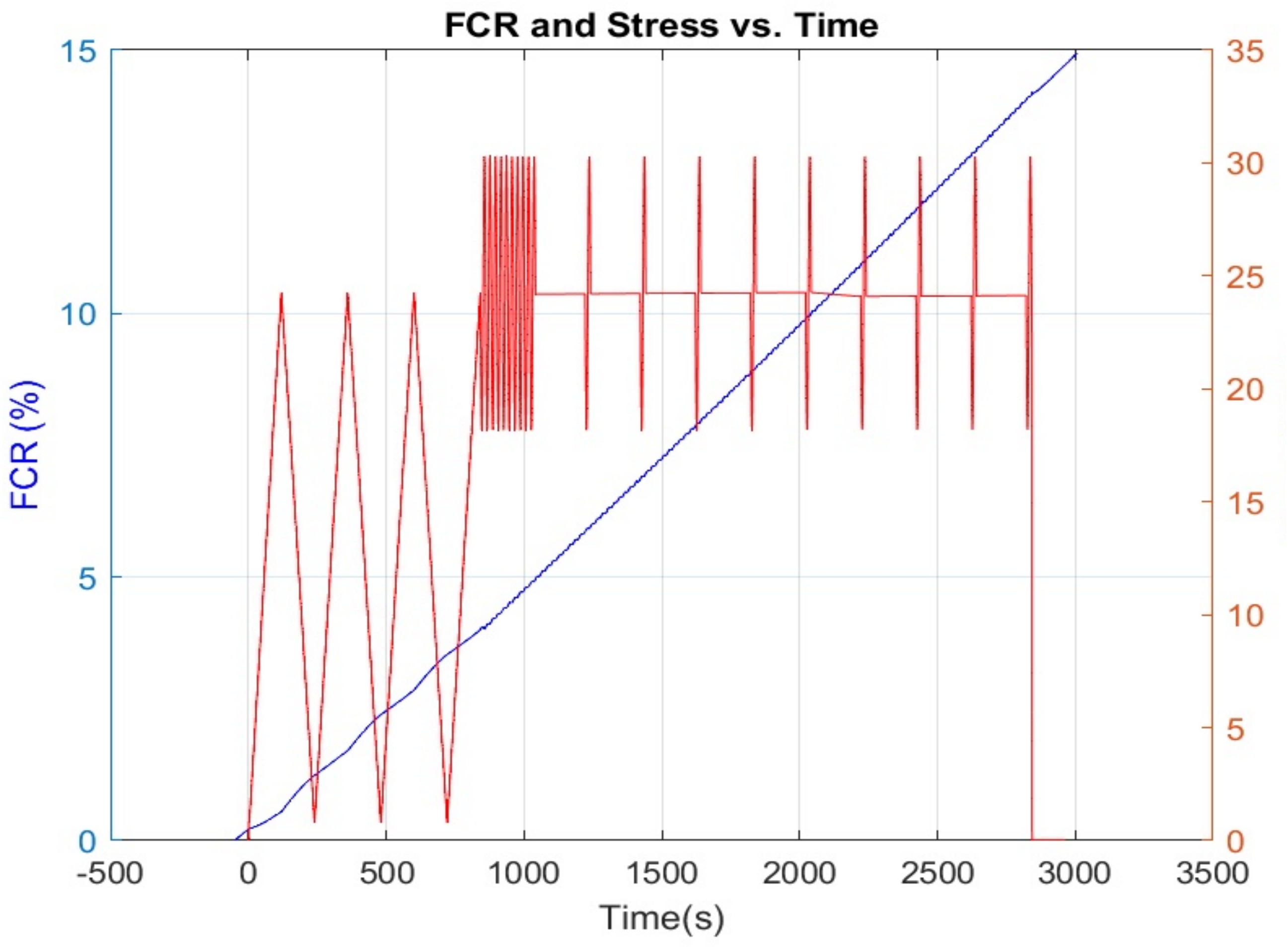

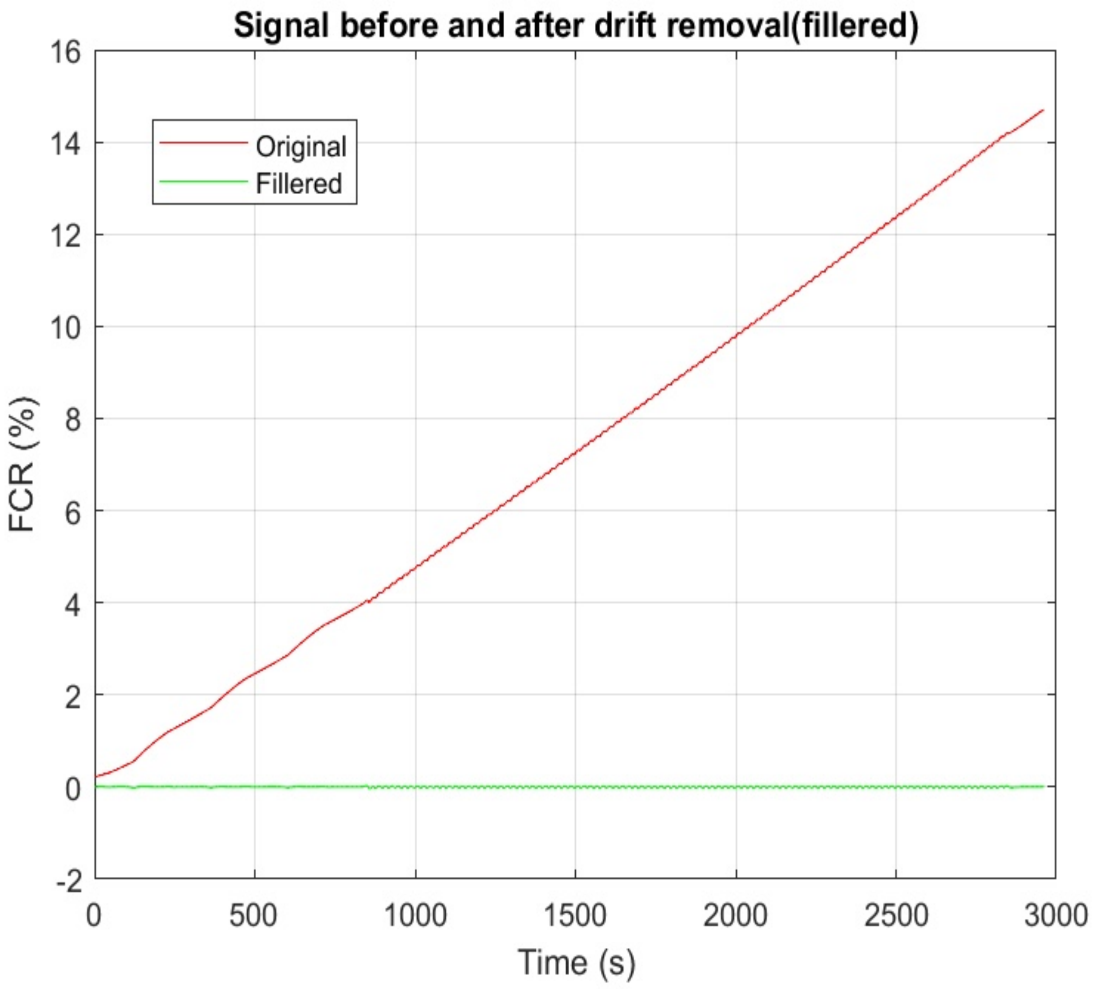

3 cycles
0.4 max loading

100 sin-shaped cycles
0.4-0.6 max loading

Signal drift ------electrical polarization

Cement-based

Geopolymer with graphite and recycled tyre steel fibres

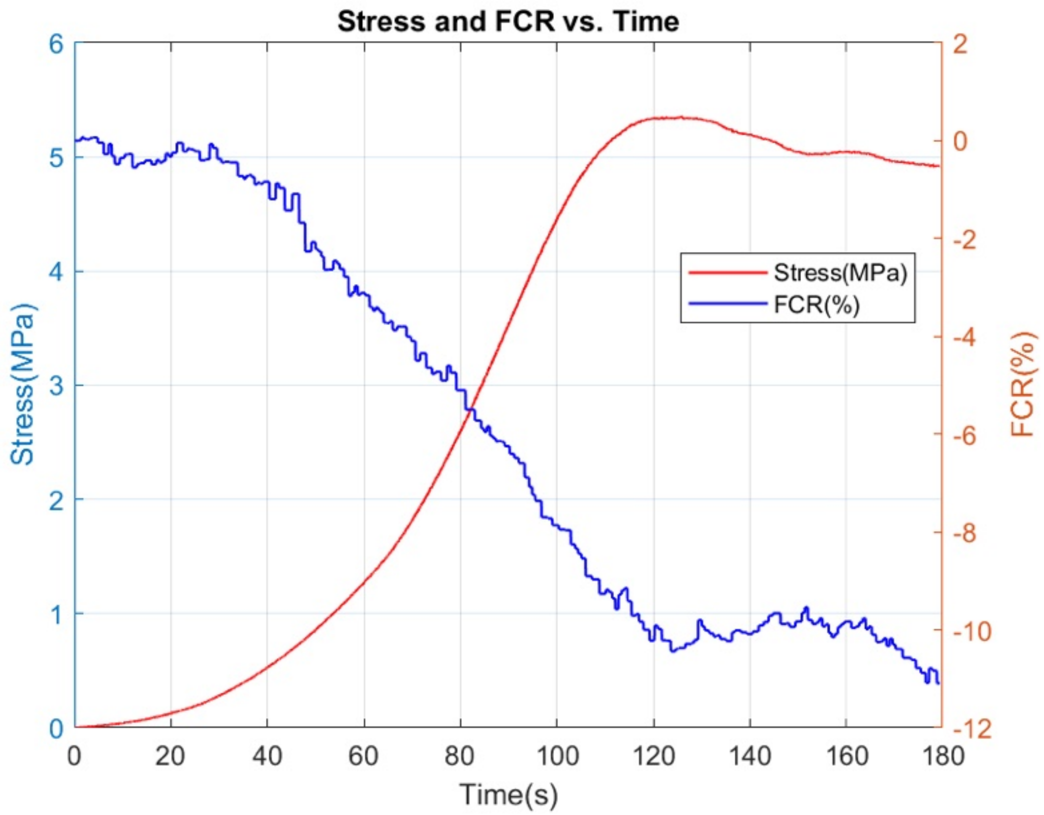

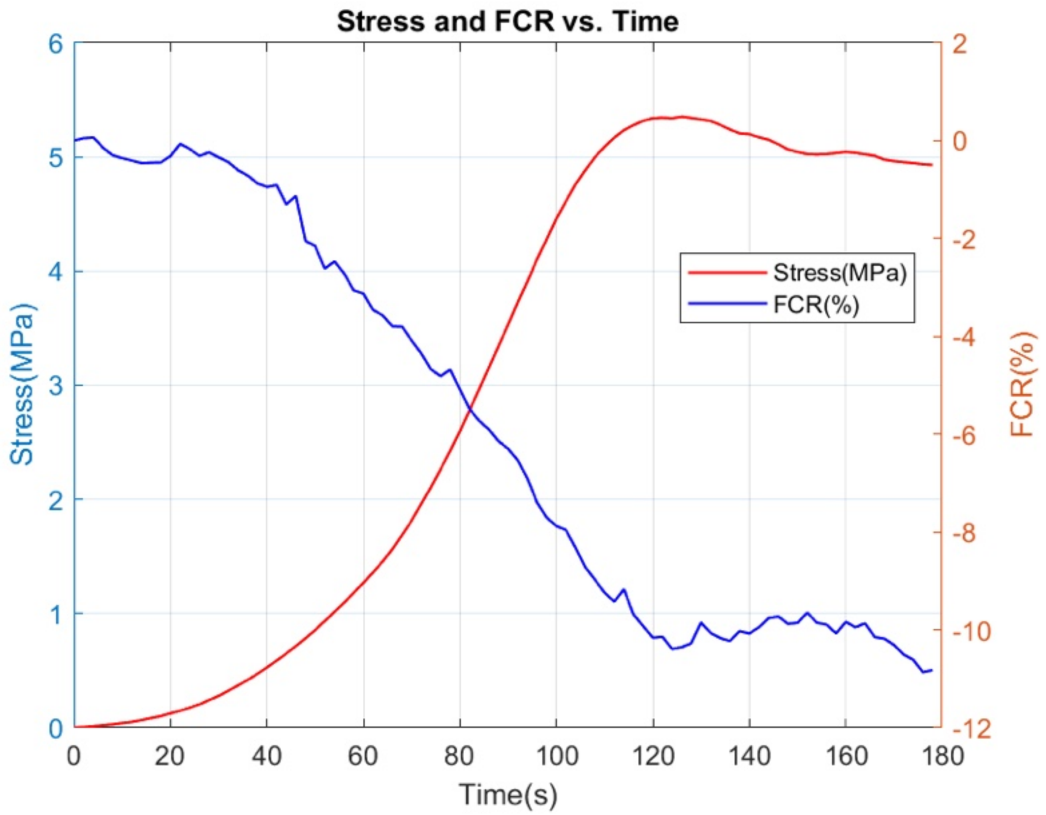

F30G70A15B650 (M13) + 5% graphite at 7days

Original data

After remove noise

F30G70A15B650 (M13) + 5% graphite at 7days

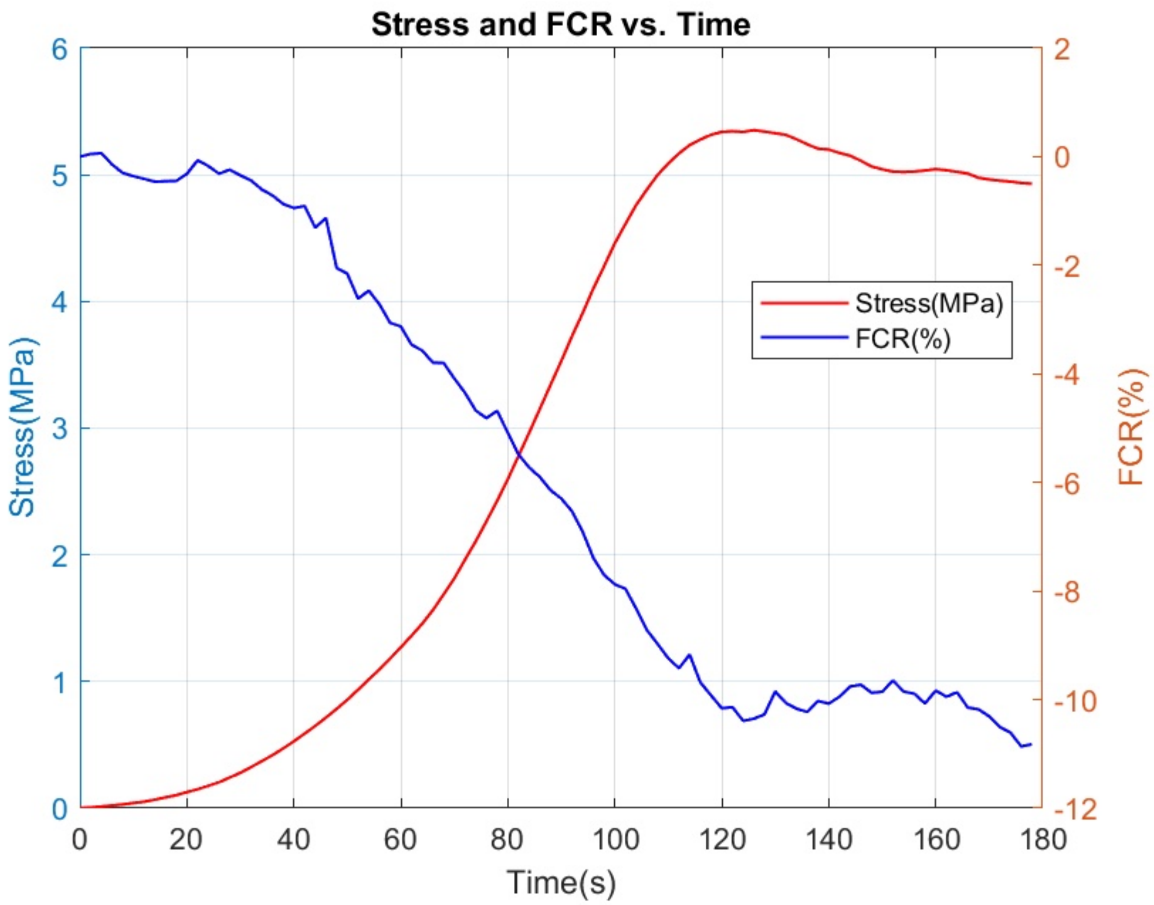

F30G70A15B650 (M13) + 5% steel fibres at 7days

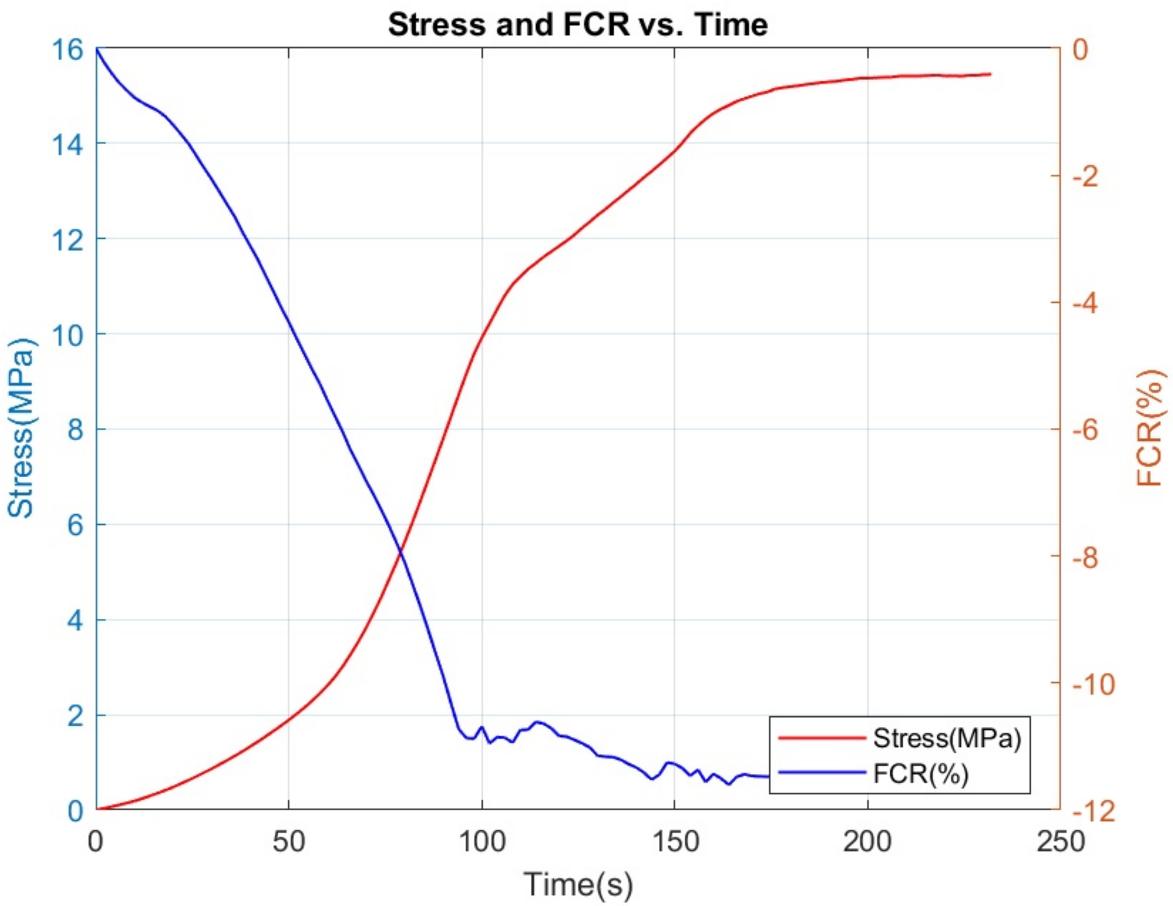

Geopolymer with graphite and recycled tyre steel fibres

FCR(%) to 20MPa at 7 days

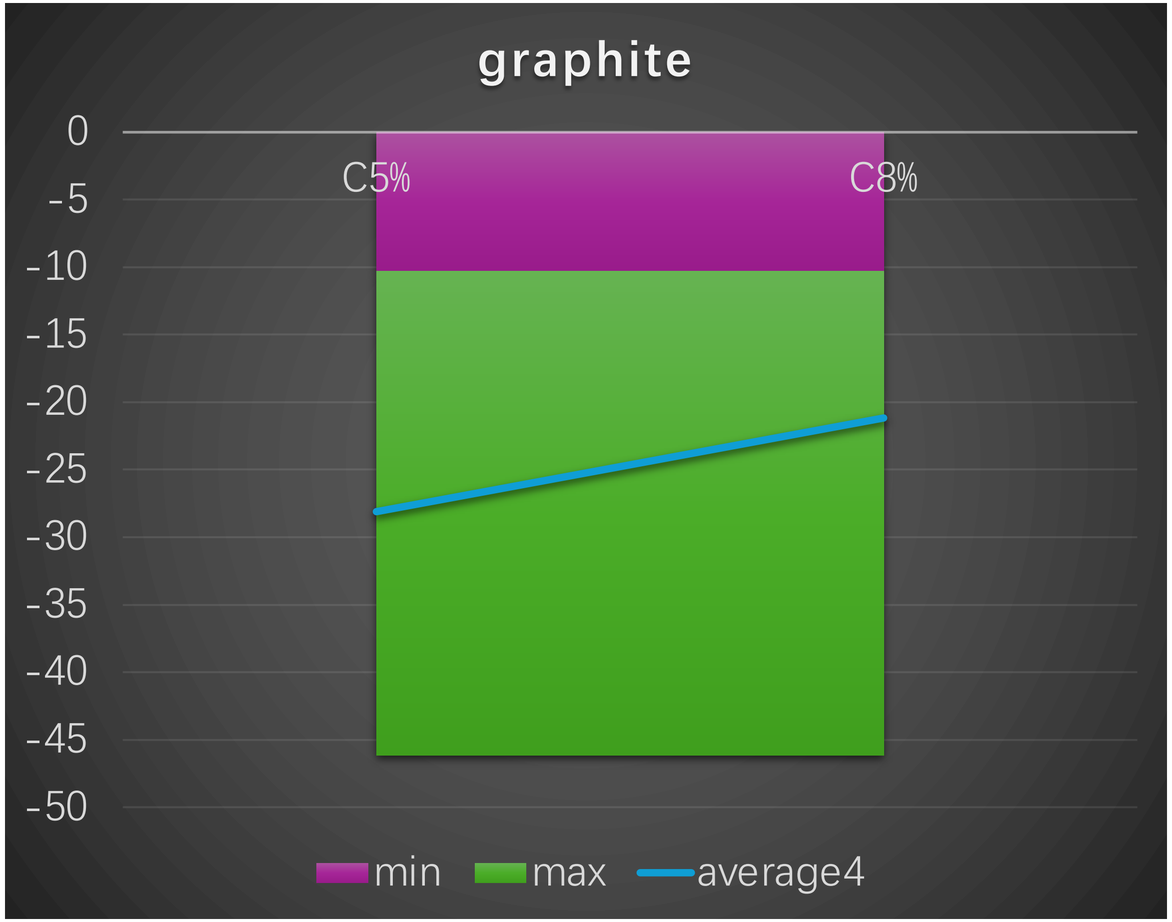

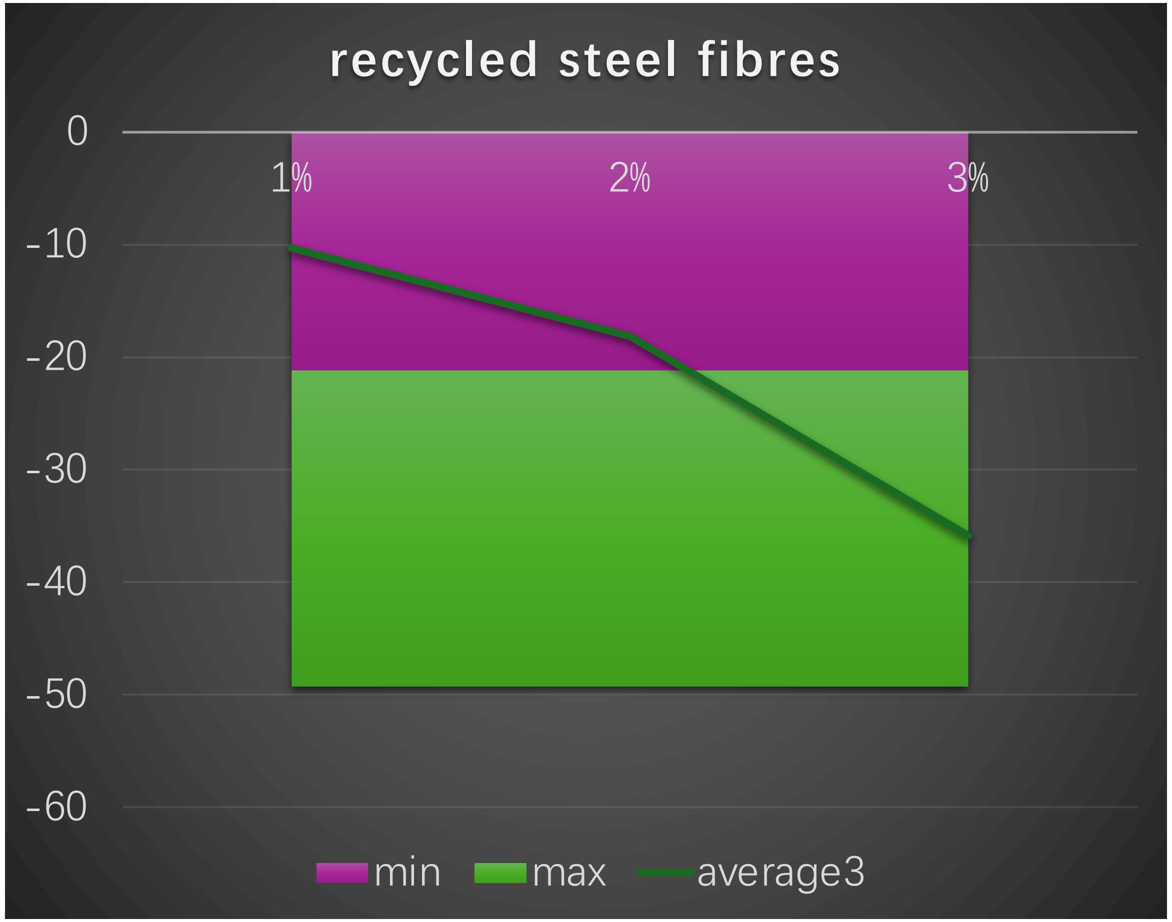

Self-sensing performance under cyclic loading at other ages? To be continued

Geopolymer VS cement-based concrete in self-sensing application

Matrix

Cement-based

- Can design mixes with water/binder ratio according to target strength
- Normal setting time
- Less iron path inside and less conductivity
- Less sensitive
- Need water curing normally
- Exist polarization

Geopolymer

- Can achieve target strength but needs more trial tests
- Less setting time due to heat release
- **More iron path inside and more conductivity**
- **More sensitive to stress changes**
- Normally needs sealed air curing
- Exist polarization

Fillers

With graphite

- **Better distribution**
- Negative to flowability
- Negative to strength
- **Less cracks after loading**

With steel fibres

- Poor distribution
- Negative to flowability
- **Negative/positive to strength depends on the percentage**
- More tiny cracks after loading
- **More conductive**

Thank you for your attention!

Contact:
Email: chenmeng.zhang@surrey.ac.uk
https://www.linkedin.com/in/chenmeng-zhang/

Funded by University of Surrey and China Scholarship Council

References

Han, B., Yu, X. and Ou, J. 2014b. Structures of Self-Sensing Concrete. Self-Sensing Concrete in Smart Structures, pp. 1–11. doi: 10.1016/B978-0-12-800517-0.00001-0.

Piro, N.S., Mohammed, A.S. and Hamad, S.M. 2023. Compressive strength and piezoresistivity of smart cement paste modified with waste steel slag. Journal of Building Engineering 70. doi: 10.1016/j.jobe.2023.106393.

Vlachakis, C., Perry, M. and Biondi, L. 2020. Self-Sensing Alkali-Activated Materials: A Review. Minerals 2020, Vol. 10, Page 885 10(10), p. 885. Available at: https://www.mdpi.com/2075-163X/10/10/885/htm [Accessed: 25 March 2022]

Mizerová, C., Kusák, I., Topolář, L., Schmid, P. and Rovnaník, P. 2021. Self-Sensing Properties of Fly Ash Geopolymer Doped with Carbon Black under Compression. Materials 2021, Vol. 14, Page 4350 14(16), p. 4350. Available at: https://www.mdpi.com/1996-1944/14/16/4350/htm [Accessed: 11 March 2024].

Ferdiansyah, T., Balayssac, J.P. and Turatsinze, A. 2022. An Experimental Approach for Characterisation of Concrete Damage Using the Wheatstone Bridge Circuit. International Journal of Civil Engineering 20(1). doi: 10.1007/s40999-021-00659-z.

Shahzad, S., Toumi, A., Balayssac, J.P., Turatsinze, A. and Mazars, V. 2022. Cementitious composites incorporating Multi-Walled Carbon Nanotubes (MWCNTs): effects of annealing and other dispersion methods on the electrical and mechanical properties. Materiaux et Techniques 110(1). doi: 10.1051/mattech/2022020.

Han, B., Yu, X. and Ou, J. 2014a. Applications of Self-Sensing Concrete. In: Self-Sensing Concrete in Smart Structures. Elsevier, pp. 189–230. doi: 10.1016/b978-0-12-800517-0.00007-1.

García-Macías E, Ubertini F. 2019. Earthquake-induced damage detection and localization in masonry structures using smart bricks and Kriging strain reconstruction: A numerical study. Earthquake Engng Struct Dyn. 48: 548–569. https://doi.org/10.1002/eqe.3148

Han, B., Ding, S., and Yu, X. 2015. Intrinsic self-sensing concrete and structures: A review. Measurement, 59:110–128

Zhang. C., Bompa, D.V., Biswal, S. and Wang, Y. 2024. Performance of one-part alkali-activated materials incorporating fly ash and slag. In Proceedings of the 15th fib International PhD Symposium in Civil Engineering, Budapest, Hungary, 28–30 August 2024.